

UNIVERSITY OF NAPLES "FEDERICO II"



XXV Cycle

PhD Program in Neuroscience

School of Molecular Medicine

**Characterization of Carbonic Anhydrases in
Models of Neuronal Differentiation and in the
Nematode *Caenorhabditis elegans***

**Coordinator:
Prof. Lucio Annunziato**

**Tutor:
Prof. Nicola Zambrano**

**PhD student:
Monica Vitale**

ACADEMIC YEAR 2011-2012

*To my darling husband Basilio
and my precious son Emanuele.
I love you.*

ABSTRACT	5
1. INTRODUCTION	6
1.1 Carbonic Anhydrases	6
1.1.1 CA9 Gene and Its Products.....	7
1.1.2 CA IX – Protein Functions in Hypoxic Cells.....	12
1.2 Nucleocytoplasmic transport.....	17
1.2.1 Nuclear import.....	18
1.2.2 Nuclear export.....	20
1.2.3 The Ran cycle	22
1.3 The Ubiquitin-Proteasome system.....	24
1.4 Experimental models	27
1.4.1 Embryonic Stem cells.....	27
1.4.2 <i>Caenorhabditis elegans</i> as animal model.....	30
1.4.3 <i>C. elegans</i> and the oxygen deprivation response.....	31
1.4.4 <i>C. elegans</i> carbonic anhydrases	32
2. AIMS OF THE THESIS PROJECT	35
3. RESULTS	36
3.1 Characterization of CA IX interactome.....	36
3.2 CA IX expression and subcellular distribution in cellular models of neuronal differentiation	41
3.3 Analysis of putative nuclear localization and nuclear export signals in the CA IX sequence.....	46
3.4 CA IX is bound to the chromatin of the 45S rRNA precursor	52
3.5 Functional validation of CA IX-CAND1 interaction	54
3.6 Possible role of CA IX and CAND1 in survival of hypoxic neuroblastoma cells	57
3.7 Carbonic anhydrases in <i>C. elegans</i>	60

4. DISCUSSION	65
5. MATERIALS AND METHODS	70
5.1 Cell lines, Caenorhabditis elegans maintenance and experimental treatments.....	70
5.2 DNA constructs.....	71
5.3 Cell lysates preparation, interactome characterization and mass spectrometry protein identification	74
5.4 Bioinformatic analysis	74
5.5 Antibodies, interaction assays and western blot analysis	75
5.6 Fluorescence and immunofluorescence analyses	75
5.7 Chromatin Immunoprecipitation	76
5.8 Analysis of cell death	77
5.9 Measuring Egg Laying and Embryonic Lethality in C.elegans	78
6. ACKNOWLEDGEMENTS	79
7. REFERENCES	80

ABSTRACT

CA IX is a member of the carbonic anhydrase family of enzymes. It is a well known marker of hypoxia and it is involved in pH and survival regulation in hypoxic cells. The main aim of my PhD project was to identify molecular interactors of CA IX and, based on the knowledge of its ligands, to contribute to functional characterization of CA IX in neuronal cells.

A complex protein network of novel CA IX interactors has been highlighted: several proteins of the nucleo-cytoplasmatic machinery have been found to bind CA IX under hypoxic condition; many of the CA IX protein interactors belong to the family of the ARM and HEAT-repeat containing proteins. Both in normoxic and hypoxic conditions CA IX also interacts with Cullin-associated NEDD8-dissociated protein 1 (CAND1), which is a nuclear HEAT/ARM-containing protein that is involved in gene transcription and assembly of the SCF E3 ubiquitine ligase complexes.

Immunofluorescence (IF) analysis demonstrated an accumulation of CA IX in the nuclei of neuroblastoma cell lines and in neurons derived from murine ESCs. Putative NLS/NES sequences were identified in the CA IX protein sequence; IF analysis showed that they were able to affect distribution of the reporter protein GFP inside the cell.

Collectively, these data suggest that subcellular localization and functions of CA IX are more complex than previously thought. CA IX may have intracellular functions different from those already known at the plasma membrane. A nuclear function for CA IX is in fact suggested by its localization on transcribed chromatin.

Finally, the nematode *Caenorhabditis elegans* was used as an animal model, in order to characterize the function of two carbonic anhydrases of the worm, namely, *cah-5* and *cah-6*, during hypoxic and anoxic stresses. Although preliminary, the observed phenotypes allow to predict fundamental roles for carbonic anhydrases *in vivo*.

1. INTRODUCTION

1.1 Carbonic Anhydrases

The carbonic anhydrases, or carbonate dehydratases (CAs), are ubiquitous metallo – enzymes present in prokaryotes and eukaryotes, encoded by five evolutionarily unrelated gene families. They are divided into α -CAs (present in vertebrates, bacteria, algae and green plants), β -CAs (in bacteria, algae and chloroplasts of monocotyledons and dicotyledons), γ -CAs (in *Archea* and some bacteria) δ -CAs and ζ -CAs (in some marine diatoms) ¹⁻⁷.

All human CAs (hCAs) belong to the α -class, and differ for their subcellular localization, tissue distribution and catalytic activity: CA I, II, III, VII and XIII are cytosolic enzymes, CA IV, IX, XII and XIV are associated to the cell membrane, CA VA and VB occur in the mitochondria; finally, CA VI is secreted in saliva and milk ⁸.

Some isoforms have an intracellular catalytic domain (CA I, II, III), others indeed possess an extracellular catalytic domain (CAIV, IX, XII, XIV). Finally, CA VIII, X, XI are better defined as "CA-related proteins", because they have no catalytic activity (Figure 1).

The carbonic anhydrases catalyze the reversible reaction $\text{CO}_2 + \text{H}_2\text{O} \leftrightarrow \text{HCO}_3^- + \text{H}^+$ with the participation of a Zn^{++} ion, present in the active site in almost all CAs, that is essential for catalysis. This reaction is involved in many physiological and pathological processes such as pH and CO_2 homeostasis, respiration and transport of CO_2 , bone resorption, calcification, electrolytes secretion in various organs and tissues, gluconeogenesis, lipogenesis, ureagenesis, tumorigenicity ⁹⁻¹². For this reason, many CAs are considered possible therapeutic targets in order to treat various diseases including glaucoma, obesity, cancer, epilepsy and osteoporosis ¹³.

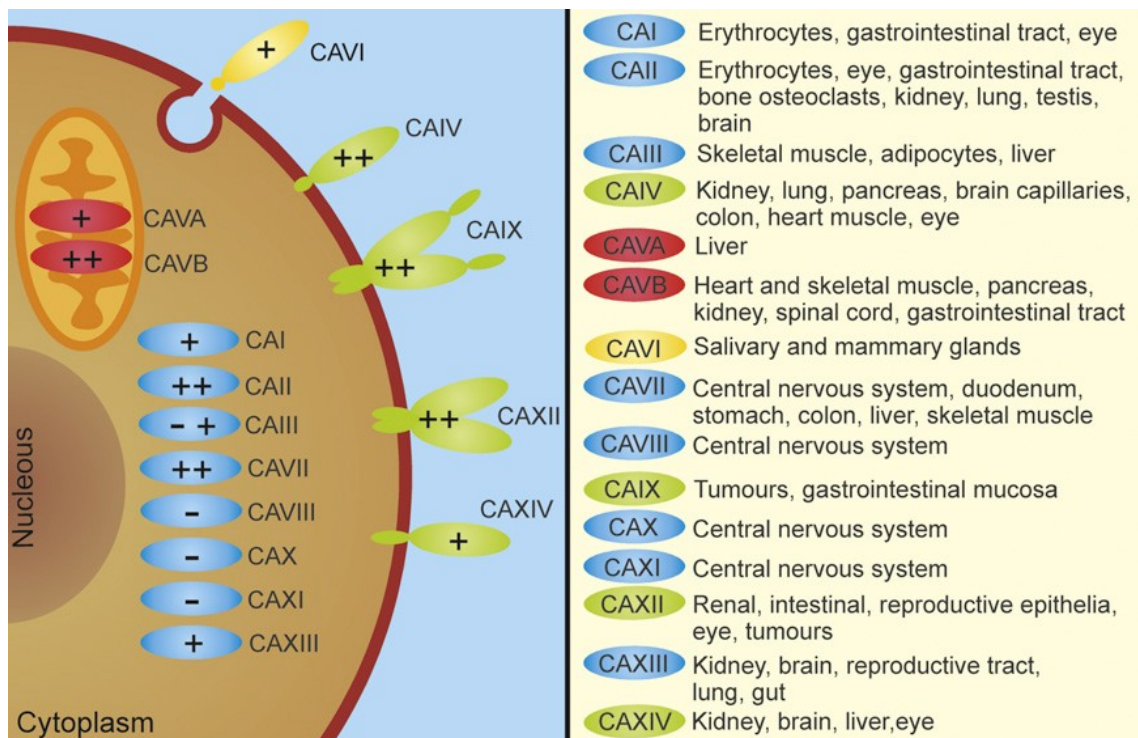


Figure 1. Schematic representation of the 15 members of human α -Carbonic Anhydrase family. The cytosolic CAs and the mitochondrial CA VA and VB only possess a CA domain; the membrane-associated CA IV, IX, XII and XIV have a transmembrane domain and, with the exception of CA IV, a cytoplasmic tail; CA IX is the only isozyme with a N-terminal proteoglycan-like domain; CA VI is secreted.. (Truppo *et al.*; *Bioorg. Med. Chem. Lett.* 2012, 22, 1560–1564).

1.1.1 CA9 Gene and Its Products

CA IX is a peculiar member of the CA family, since it is expressed in a limited number of normal tissues (mainly in the gastrointestinal tract), whereas it is generally expressed in hypoxic tissues, where its expression is mediated by the transcription factor HIF-1¹⁴.

The gene encoding for CA IX is located in the region p12-p13 of chromosome 9, and consists of 11 exons and 10 introns. The first exon encodes the putative signal peptide and the entire PG-like domain, the exons 2-8 encode the CA domain, and finally the exons 10 and 11 encode the transmembrane region and the intracellular tail, respectively (Figure 2)^{15, 16}.

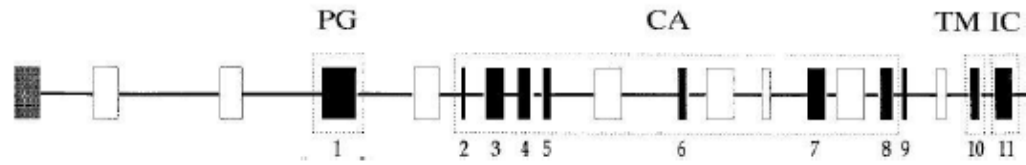


Figure 2. Map of human CA IX gene (Opavsky *et al.*; Genomics 1996, 33, 480-487).

Upon appropriate activation, *ca9* gene is transcribed into a single mRNA of 1.5 kb¹⁷. In addition to this mRNA, an alternative spliced variant, lacking exons 8/9, has been found. This variant is constitutively expressed at very low levels. This truncated form of CA IX presents a decreased enzyme activity.

The expression of CA IX is regulated at the level of its promoter (-173; +31) (Figure 3)¹⁸. The latter is characterized by six *cis*-acting elements, five with a positive and one with a negative influence on the transcription.

Immediately upstream of the transcription start site (-3; -10), an Hypoxia-Responsive Element (HRE), containing the TACGTG HIF-binding site (HBS), that is activated by HIF-1, is present. This activation is a critical element to recruit the transcriptional complex on the CA IX promoter^{14, 19}.

PR1 (-45 ; -24) and PR5 (-163; -145) are two positive *cis*-acting elements and bind SP1/SP3 factors²⁰⁻²², that can positively or negatively affect transcription²³.

Under normoxia, hypoxia and mild hypoxia (corresponding to high cell density culture), SP1/SP3 constitutively bind PR1/PR5 and this binding, when HIF-1 is activated, is critical for CA IX transcription^{20, 21, 24}.

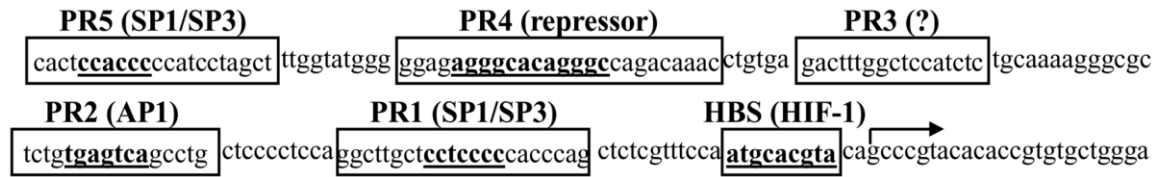


Figure 3. Sequence of the CA IX promoter and its *cis*-acting elements. PR, protected region; HBS, HIF-binding site; transcription site is indicated by arrow. Each PR is in the boxes, the cognate transcription factors are in brackets, and their binding sites are in underlined bold.

The structure of the encoded protein was initially analyzed on the basis of the sequence homology with other members of the same family ¹⁷, and then it was studied through X-ray crystallography ²⁵.

CA IX is a transmembrane protein of 459 amino acids (~58kDa) with an N-terminal signal peptide (aa 1–37), an extracellular part (aa 38–414), a transmembrane tract (aa 415–434), and an intracellular C-terminal tail (IC; aa 435–459). The extracellular part is composed of two domains: the PG-like domain (53-111) and a CA domain (135-391)(Figure 4) ^{15, 17}.

Crystallographic analysis of CA IX structure suggested a dimeric nature for this enzyme and showed that the dimer is formed through a symmetrical intermolecular disulfide bridge at the level of Cys41 placed on both monomers. These studies also show the existence of an intramolecular disulfide bond (Cys119-Cys229) and two glycosylation sites: an *N*-glycosylation (Asn309) in the catalytic domain and an *O*-glycosylation (Thr 78) near the PG domain ²⁶.

The X-ray crystallography described the catalytic domain as a globular domain in which the active site is located in a large conical cavity, that goes from the surface to the center of the protein, and a Zn⁺⁺ ion is present on the bottom of this cavity. The active site is delimited by two distinct regions made of hydrophobic (Leu91, Val121, Val131, Leu135, Leu141, Val143, Leu198 and Pro202) and hydrophilic amino acids (Arg58, Arg60, Asn62, His64, Ser65, Gln67, Thr69, and Gln92).

The different domains of CA IX were associated to specific protein functions ²⁷. The PG domain is associated with cell adhesion and intercellular communication ²⁸⁻³⁰. It also affects the enzyme activity of CA IX, ensuring a better catalytic efficiency at acid pH, indeed, the PG domain presents negatively charged amino acids that can interact with positively-charged residues that delimit the active site; this interaction may control substrate accession or participate in the proton transfer reaction ²⁵.

The catalytic CA domain is involved in cellular growth and survival ²⁷, whereas the IC tail is essential for enzyme action and for a proper plasma membrane localization. Mutagenesis of several residues in the IC region does not allow a correct membrane localization, reduces the cell-cell adhesion, alters the interaction with other proteins involved in the signal transduction and abolishes the acidification of the extracellular environment ³¹. This happens because the IC tail possesses three phosphorylation sites, two of which, namely T443 and S448, modulate the CA IX catalytic activity, while the Y449 is involved in EGFR-induced signal transduction to PI3K/Akt kinase pathway ^{32, 33}.

Recently, our work has highlighted the presence of putative nuclear localization sequences (NLS) and nuclear export sequences (NES) in the intracellular tail and transmembrane region of CA IX, respectively, that seem to drive intracellular distribution of CA IX ³⁴.

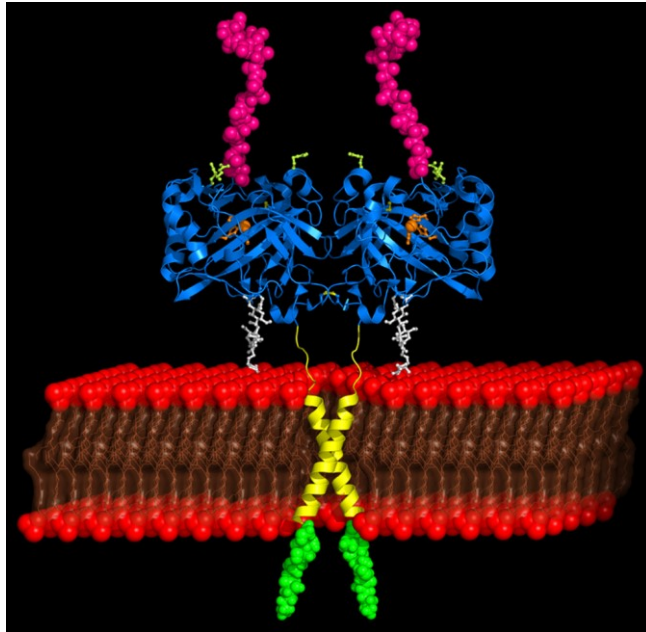


Figure 4. CA IX dimer structure, based on the X-ray crystallography data. The catalytic domain is reported in cyan, with the glycan moieties in white. The PG domain is represented in magenta, the transmembrane tract in yellow and finally, the intracellular tail in green. (Alterio *et al.*; PNAS 2009, 106, 38, 16233–16238);

1.1.2 CA IX – Protein Functions in Hypoxic Cells

Hypoxia is a state of oxygen deficiency, in tissues and cells, sufficient to impair functions of the brain and other organs.

Furthermore, hypoxia is one of the characteristics of solid tumors and correlates with the propagation of tumors, the malignancy and resistance to radio-and chemo-therapy. The metabolic changes occurring in hypoxic cells, which allow them to adapt to hypoxic stress when the oxygen tension falls below of 1-10 mmHg, are largely regulated by HIF-1.

As mentioned previously, also the expression of CA IX is regulated by the binding of HIF-1 to HRE sequences, present at the level of its promoter; in contrast to most of the other hypoxia-inducible-genes, CA IX is exclusively transactivated by HIF-1.

HIF-1 is a heterodimeric transcription factor composed of an α subunit, stabilized by O₂, and a β subunit, constitutively expressed (Figure 5). There are three α subunits (1 α , 2 α , 3 α), but only HIF-1 α is able to transactivate the CA IX promoter³⁵.

In normoxic conditions, HIF-1 α is addressed to the proteasome, through a process of ubiquitin-mediated degradation. This process is regulated by the prolyl-4-hydroxylase (PHD) that hydroxylates the Pro564 located in the oxygen-dependent degradation domain (ODDD) of HIF-1 α ; this allows the binding of the protein pVHL, belonging to the E3 ubiquitin ligase complex, which leads to degradation of HIF-1 α by the proteasome^{36, 37}. Moreover, HIF-1 α is hydroxylated at asparagine residue (Asn803) within the C-terminal transactivation domain (C-TAD) by the factor inhibiting HIF-1 (FIH-1) which prevents binding of the p300/CBP coactivator^{38, 39}. In hypoxic conditions, the hydroxylation cannot take place and pVHL cannot target HIF-1 α for degradation. HIF-1 α is free to accumulate in the nucleus where dimerizes with HIF-1 β and activates the transcription of genes that possess a HRE in the promoter (for example: VEGF, GLUT1/3, EPO1, CA IX)^{40, 41}.

There are some discrepancies between CA IX and HIF1 α expression. HIF1 α is rapidly degraded in normoxic condition and rapidly stabilized under hypoxic

conditions. This kinetic has a critical effect on the expression of HIF1 α target genes indeed, upon initiation of CA9 transcription, it takes several hours before CA IX protein is measurable. So, when the cells/tissue have only recently become hypoxic, HIF1 α is detectable, whereas CA IX not yet; alternatively in reoxygenated cells, HIF1 α is rapidly degraded, whereas CA IX (extremely stable) is still present ⁴².

In addition to hypoxia, other agents and genetic factors can inhibit the HIF-degradative pathway, inducing CA IX expression. Indeed, overexpression of CA IX is related to inactivating mutations or epigenetic silencing of VHL, even under normoxic conditions ^{14, 22, 43}.

CA IX expression correlates with the stabilization of HIF-1 α , but it also occurs in a HIF-1 α independent manner. Indeed, in high density cell cultures, the p110 subunit of PI3K can bind a specific *cis*-acting element of CA9 promoter and promote CA IX expression. This mechanism is mediated by a reduced oxygen tension (70 mm Hg), which is not sufficient to stabilize HIF-1 α ⁴⁴.

Since the CA IX expression is closely linked to hypoxic conditions, it is considered an endogenous marker of hypoxia.

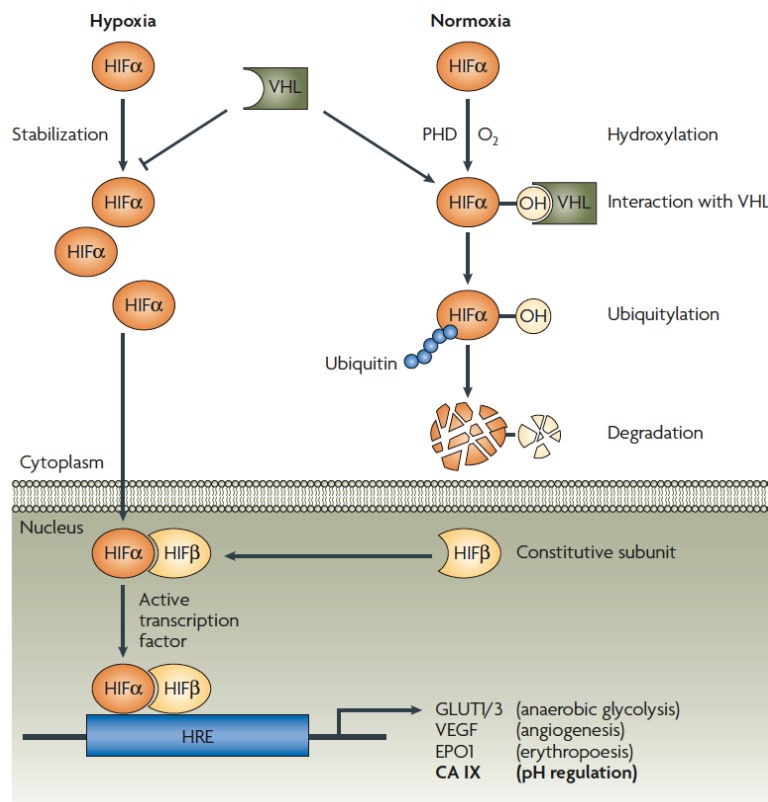


Figure 5. Mechanism of hypoxia-induced HIF1 stabilization and activation, leading to CA IX overexpression in hypoxic cells. Under normoxia, HIF1 α is hydroxylated by PHD and then bound by VHL that target HIF1 α for degradation by the ubiquitin-proteasome system. Under hypoxia, PHD is inactive, HIF α is not recognized by VHL and can move into the nucleus, where together with HIF1 β , acts as transcription factor for target genes (Supuran CT, *et al.* Nat Rev Drug Discov 2008, 7, 168-181).

In normoxic conditions, cells convert glucose in glucose-6-phosphate, that is converted to pyruvate. Pyruvate is oxidized in the mitochondria to CO₂ and H₂O, generating 38 molecules of ATP per glucose molecule. In hypoxic conditions, oxidative phosphorylation cannot take place, so the pyruvate is reduced to lactate, generating 2 molecules of ATP per glucose molecule.

However, in order to survive, hypoxic cells have to maintain a pH_i close to physiological levels, so that the pyruvate and lactate products are released into the extracellular environment. In this way, a pH gradient occurs between the

inside and outside of the cell, stabilizing an extracellular pH (pHe) value around 6, against the physiological value of 7.4 ⁴⁵.

In hypoxic cells, CA IX function consists in maintaining this pH gradient through acidification of extracellular pH (pHe) and alkalization of intracellular one, so counteracting hypoxia-induced acidosis ⁴⁶. Indeed, bicarbonate and protons produced by CA reaction contribute to further increase intracellular pH (pHi) and decrease extracellular one, respectively. More specifically, CA IX interacts with bicarbonate transporters forming metabolons ⁴⁷, that allow bicarbonate to be shuttled in the cytoplasm to buffer pHi, while the protons remain extracellularly; alternatively, bicarbonate can be transported to blood capillaries through anionic exchanger $\text{HCO}_3^-/\text{Cl}^-$ (Figure 6).

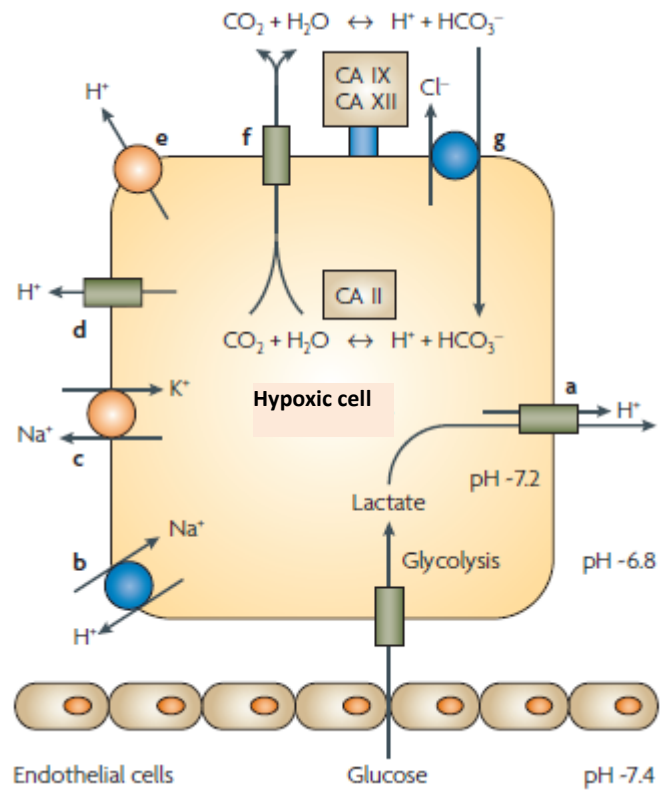


Figure 6. pH regulation within hypoxic cells. Hypoxic cells show a pH gradient characterized by acidic pH values in the extracellular microenvironment and by slightly alkaline pH values within them. (image modified from: Supuran; Nat Rev Drug Discov 2008, 7, (2), 168-81).

1.2 Nucleocytoplasmic transport

In eukaryotic cells, the separation between nucleus and cytoplasm is defined by the nuclear envelope, a double-membrane system of highly selective permeability. A continuous interchange of material between these two compartments occurs through dedicated transport channels, that spans the nuclear envelope, namely the nuclear pore complex (NPC).

The NPC is characterized by three substructures: the cytoplasmic filaments, a central core and the nuclear basket. The central core connects cytoplasmic ring to nuclear one through eight spokes, forming an aqueous channel. Each NPC is composed of about thirty different proteins, called nucleoporins, each of which is present in a large number of copies ^{48, 49}.

The nucleoporins are divided into three groups: a first group includes transmembrane nucleoporins, which allow to anchor the NPC to the nuclear envelope; a second group consists of FG-nucleoporins, characterized by phenylalanine and glycine repeats (FG repeats), which possess binding sites for karyopherins; finally, a third group includes structural nucleoporins, which form a scaffold that interacts with transmembrane nucleoporins and FG-nucleoporins ⁵⁰.

Small molecules (up to 20 kDa), soluble in water, can diffuse through the channels of the NPC, instead, larger molecules are actively transported through hydrolysis of GTP, catalyzed by the protein Ran, and transport by the karyopherins- β .

The karyopherins- β belong to a family of proteins of about 100 kDa; in humans, about 20 proteins have been identified, that are able to recognize the cargo proteins, thanks to their ability to change conformation. All karyopherins- β contain 19-20 helical HEAT repeats arranged into super-helical or ring-like structures ⁵¹. The karyopherins- β that mediate nuclear import are generally known as importins, whereas those mediating nuclear export are known as exportins.

Importin α directly bind the cargo protein and is characterized by a critical region for recognition of cargo. This region is made up of 10 armadillo (ARM) repeats. The ARM repeat is an ~40 amino acids motif that form three α -helices (H1, H2, H3). The H3 helices form the inner concave surface of the importin α ⁵¹.

1.2.1 Nuclear import

The molecules that have to be transported into the nucleus possess a nuclear localization signal (NLS), classically represented by three or five positively charged amino acid residues. The NLS can be monopartite (containing one cluster of positively charged amino acids), as in case of the large T antigen of the SV40 virus (PKKKRKV), or bipartite (possessing two clusters of positively charged amino acids), such as that of nucleoplasmin (AVKRPAATKKAGQAKKKKLD)^{52, 53}.

In the cytoplasm, the cargo molecule binds, through the NLS, the ten ARM domains of the importin- α . At the N-terminus, importin α possess a importin β - binding (IBB) domain by which bind importin β , forming a ternary NLS-Imp α / β complex (Figure 7). This complex is transported in the nucleus via the NCP, where RanGTP binds importin- β , causing cargo dissociation.

The adaptor importin α returns in the cytoplasm by a dedicated receptor, the exportin Cse/CAS, upon hydrolysis of RanGTP to RanGDP.

The importin- β drives the transport to the nucleus by interacting with the repetitions FG of nucleoporins. In a limited number of cases, importin β binds cargo directly. In this case, release of cargo in the nucleus is determined by mutually exclusive binding of cargo and RanGTP, as their binding site, at the N-terminus arch of importin- β , are almost completely overlapping⁵⁴.

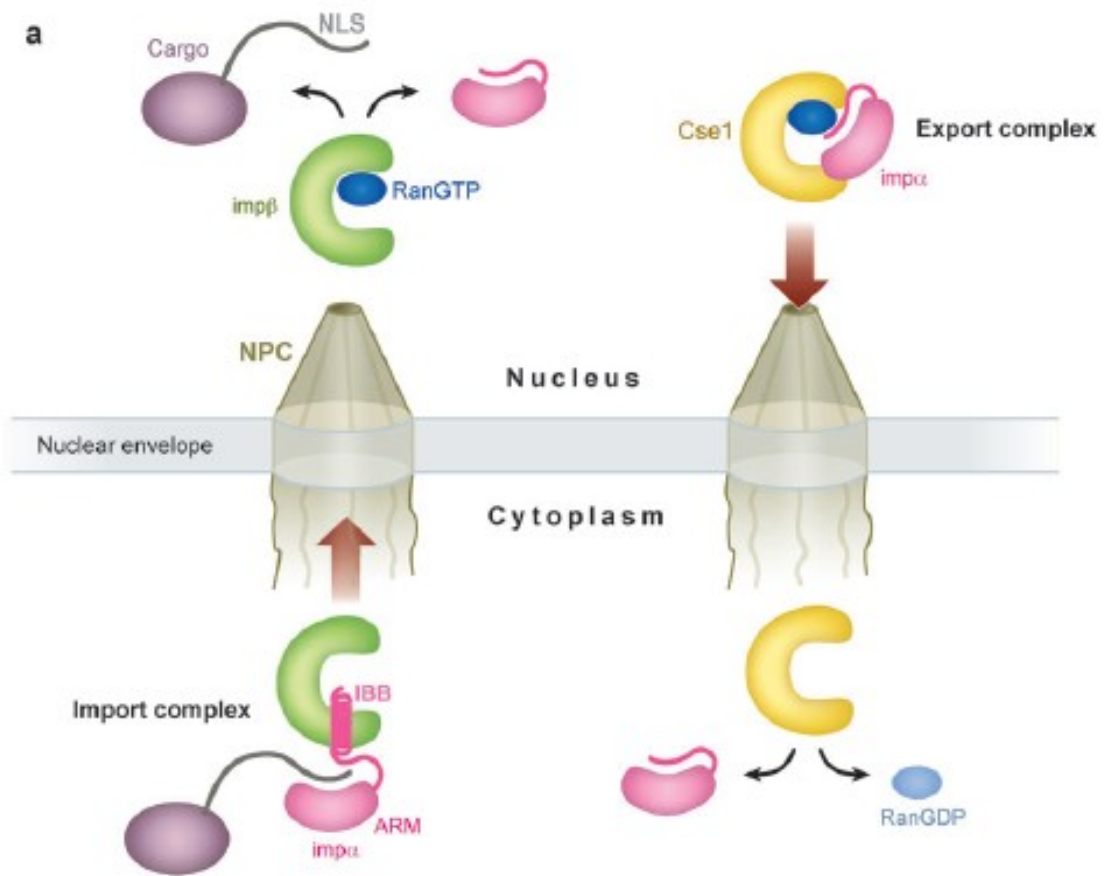


Figure 7. Schematic representation of nuclear import. The adaptor molecule importin α ($imp\alpha$) recognizes the NLS sequence present in the cargo to be transported, via its armadillo-repeat domain (ARM). The importin β -binding (IBB) domain of importin α binds in a helical conformation to importin β ($imp\beta$). The cargo- $imp\alpha/\beta$ complex is transported to the nucleus, via the nuclear pore complex (NPC). In the nucleus, the ternary complex is dissociated upon the formation of importin β -RanGTP complex. $Imp\alpha$ is recycled back by the exportin Cse1/CAS (Cook *et al.*; Annu. Rev. Biochem. 2007, 76, 647–71).

1.2.2 Nuclear export

In the nucleus, in the presence of RanGTP, the cargo proteins are bound by exportins and they are released in the cytoplasm upon conversion of RanGTP into RanGDP (Figure 8).

One of the most studied exportin is XPO1 (also known as exportin-1 or CRM1). Generally, exportin-1 cargoes contain a nuclear export signal (NES), which is rich in hydrophobic amino acids, such as leucine.

The crystal structure of C-terminal fragment of exportin-1 shows that this protein presents 20 HEAT repeats. These HEAT repeats are arranged into a ring and by an allosteric mechanism, allow exportin-1 to interact with the NES sequences of the cargoes and with the nuclear pore complexes, as well as happens for importins.

In humans, the activity of XPO1 can be inhibited by Leptomycin B (LMB), an unsaturated fatty acid that blocks the XPO1 binding site for NESs, by covalent modification at a cysteine residue ⁵⁵.

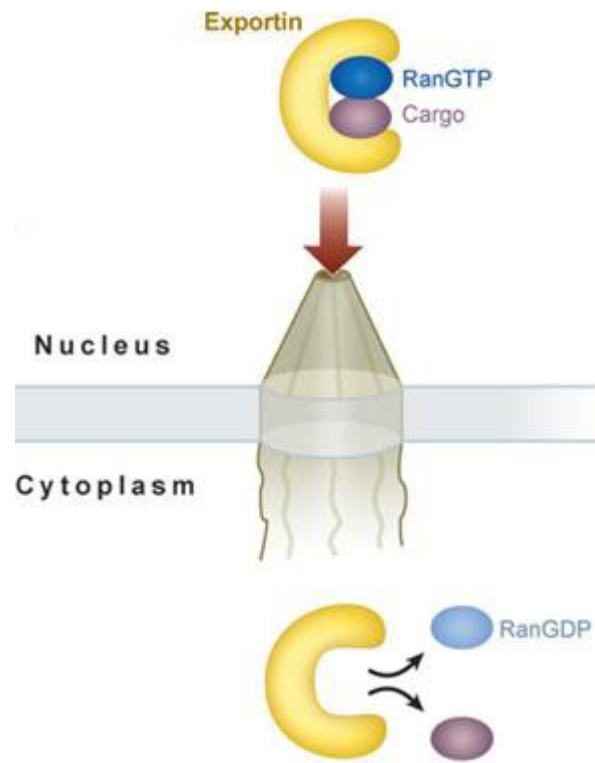


Figure 8. Schematic of nuclear export. In the nucleus, an exportin binds both cargo and RanGTP and release them in the cytoplasm, upon conversion of RanGTP into RanGDP (Cook *et al.*; Annu. Rev. Biochem. 2007, 76, 647–71).

1.2.3 The Ran cycle

Transport directionality and karyopherin β – cargo interaction are regulated by the RanGTPase nucleotide cycle (Figure 9) ⁵⁶.

Ran is a small monomeric GTPase, belonging to the Ras superfamily, that is able to hydrolyze the GTP to GDP. There is a different distribution of Ran between nucleus and cytoplasm: RanGTP is concentrated in the nucleus, while RanGDP is more present in the cytoplasm. This compartmentalization depends on the activity of proteins that control the nucleotide state of Ran, indeed to hydrolyze GTP, Ran needs a Ran GTPase-activating protein (RanGAP), that is present in the cytoplasm and accelerates the hydrolysis of GTP to GDP. Conversely, in the nucleus, a guanine nucleotide exchange factor (GEF) (also known as regulator of chromosome condensation 1 or RCC1) increases the rate of nucleotide dissociation, promoting rapid GDP release after GTP hydrolysis and reloading of the G protein with GTP.

RanGAP needs RanBPs (Ran-binding proteins) cofactors to increase GTPase activity of Ran. RanBP2 interacts with the cargo-importin- α/β complex at the level of NPC, so Ran-GTP binds importin- β causing a conformational change that induces the release of the protein transported and importin- α . The complex importin- β /Ran-GTP is carried in the cytoplasm, where Ran-GAP hydrolyzes GTP to GDP and the complex dissociates. Following hydrolysis, Ran-GDP is associated with protein NTF2 (nuclear transport factor 2) and is recycled back to the nucleus ⁵⁷.

In the nuclear export, the binding of Ran-GTP to exportin stabilizes the complex XPO1/protein. This complex is transported into the cytoplasm, where it is dissociated by the action of Ran-GAP, and the exportin returns in the nucleus. Even if importin- α doesn't have a classical NES, it is recycled in the cytoplasm, by the Cse-1 ⁵⁵.

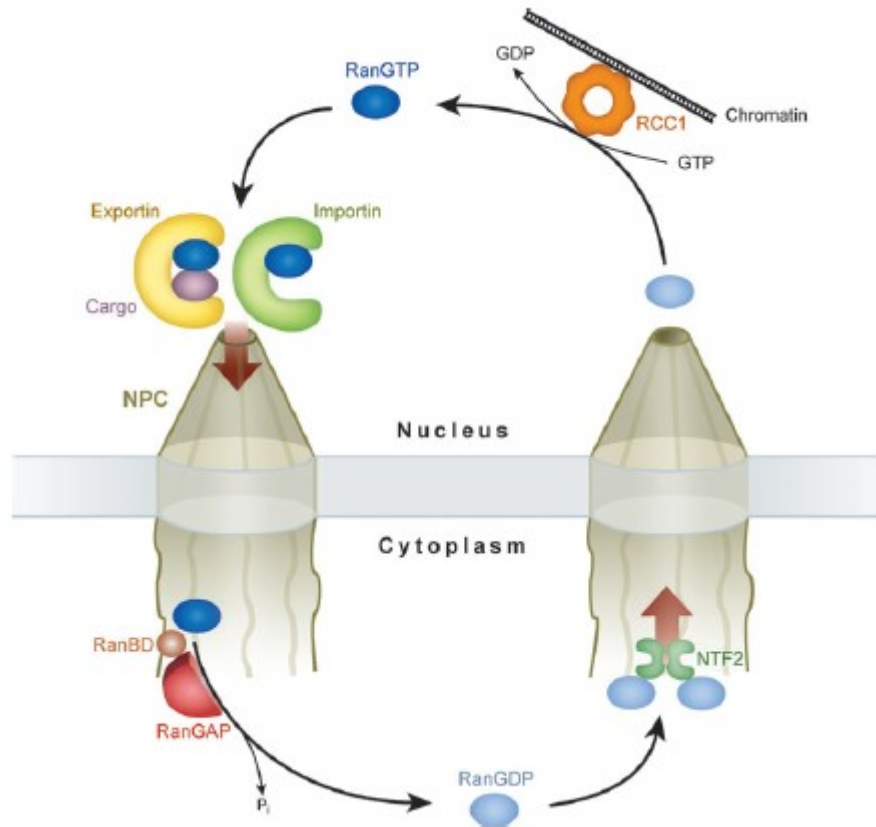


Figure 9. Schematic description of the Ran cycle. In the cytosol, the high concentration of RanGDP is maintained by RanGAP, which is bound to the cytoplasmic fibrils of the nuclear pore complex. It acts on the RanGTP that enters the cytoplasm (via binding to exportins and importins). In the nucleus, the high concentration of RanGTP is maintained by RanGEF, a chromatin-bound guanine exchange factor (RCC1), which acts on the RanGDP, that enters the nucleus with its dedicated transport factor nuclear transport factor 2 (NTF2) (Cook *et al.*; Annu. Rev. Biochem. 2007, 76, 647–71).

1.3 The Ubiquitin-Proteasome system

In the cell, in order to maintain intracellular protein homeostasis, proteins are continuously synthesized and degraded. The ubiquitin proteasome system control the degradation of the majority of intracellular proteins and consist of two principal steps. The first one is the covalent assembly of a chain of the small protein ubiquitin on the target protein and is catalyzed by the sequential action of three enzyme (Figure 10) ^{58, 59}.

In the first step, ubiquitin is activated by the ubiquitin-activating enzyme (E1), in the second one it is transferred to ubiquitin-conjugating enzyme (E2). E2 charged with ubiquitin cooperates with ubiquitin ligase (E3), to ubiquitylate the target protein. Generally, several ubiquitins are added to a protein forming an ubiquitin chain ⁶⁰.

In the second step, the energy-dependent proteolysis of the ubiquitin chain-triggered protein occurs by the 26S proteasome complex. The 26 proteasome complex is composed by the 20S proteasome and by a regulatory component, the 19S cap, that contains several ATPase subunits and other subunits involved in the action of the 26 proteasome on ubiquitylated proteins. Polyubiquitylated proteins are usually degraded by the 26 proteasome complex through an ATP-dependent reaction that produces different types of products: free peptides, short peptides, still ubiquitylated and polyubiquitin chains. These last two products are converted to free and reusable ubiquitin by the action of ubiquitin-C-terminal hydrolases or isopeptidases (Figure 10) ⁶¹.

The SCF complex is a multisubunit ubiquitin ligase and it consists of three invariant subunits, Skp1, Cul1 and Rbx1 (also known as Roc1 or RING) and a variable F- box protein (FBP) subunit. Cul1 and Rbx1 are the catalytic core, Skp1 is an adaptor protein which interacts with a FBP. FBPs are the subunits that recognize and recruit the substrates in a protein-specific manner ⁶².

The catalytic core (Cul1-Rbx1) cycles between an assembled, active state and a disassembled, inactive state (Figure 11). When Cul1 is conjugated with FBP-Skp1 and with the ubiquitin-like modifier Nedd8 at Lys720 (neddylation), the

enzyme is active, indeed the neddylation causes a conformational change in the cullin and Rbx1 and increases ubiquitin ligase activity.

Inactivation of SCF occurs by deconjugation of Nedd8 (deneddylation) by the COP9 signalosome complex (CSN)⁶³. Once deneddylated, Cul1 docks the sequestration factor CAND1/TIP120A, which dislocates FBP-Skp1 and making inactive the complex⁶⁴. Because CAND1 partially occludes both the FBP-Skp1 binding site and Lys720 on Cul1, the active and inactive states of CUL1 are mutually exclusive. The combined action of Nedd8-conjugating enzymes and FBP-SKP1 dissociates CAND1, resulting in the reformation of an intact, Nedd8-conjugated SCF complex^{65, 66}.

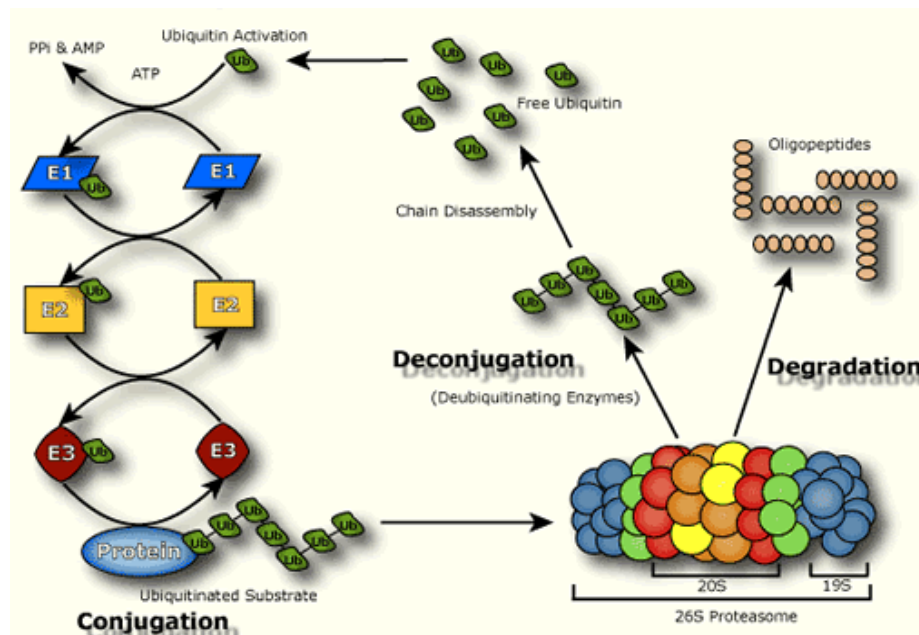


Figure 10. Ubiquitin cycle and protein degradation. Degradation of a protein via the ubiquitin proteasome pathway (UPP) involves two discrete and successive steps: tagging of the substrate protein by the covalent attachment of multiple ubiquitin molecules; and the subsequent degradation of the tagged protein by the 26S proteasome, composed of the catalytic 20S core and the 19S regulator.

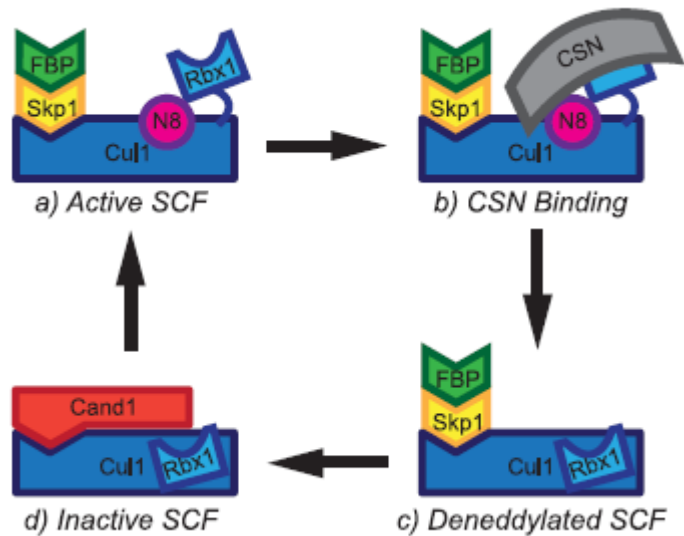


Figure 11. The Cul1 Cycle. a) Cul1 complexed with FBP-Skp1 and covalently modified with Nedd8 (N8) represents an active SCF. b) and c), Inactivation of SCF initiates when CSN binds active SCF and deconjugates Nedd8, returning the RING subunit Rbx1 to its inactive configuration. D), Cand1 dislocates FBP-Skp1 and binds Cul1, forming an inactive Cand1-Cul1 complex. Restoration of an active SCF complex is brought upon by the combined action of Nedd8-conjugating enzymes and FBP-Skp1. Conjugation of Nedd8 causes a major conformational change in Cul1 and E2-recruiting Rbx1. This dynamic cycle of Cul1 is thought to enable a rapid sampling of the steady-state FBP-Skp1 population ⁶⁷.

Mutations in either the N- or C-terminal region of both CAND1 and Cul1 disrupt their binding, suggesting that their optimal interactions require the full-length sequences of both proteins. Moreover, CAND1 does not coexist with any detectable SKP1 or F-box proteins.

CAND-1 is a nearly all-helical solenoid protein, consisting of 27 tandem HEAT repeats. Collectively, these repeats form an unusually superhelical structure with intimately coils around Cul1, making multiple intermolecular contacts ⁶⁴.

1.4 Experimental models

1.4.1 Embryonic Stem cells

Mouse embryonic stem cells (ESCs) are pluripotent cells derived from the inner cell mass (ICM) of the preimplantation embryo at the blastocyst-stage^{68, 69}. ESCs possess two unique characteristics that distinguish them from all other organ-specific stem cells identified to date. First, in culture, they can be maintained and expanded as pure populations of undifferentiated cells for extended periods of time, retaining a normal karyotype.

Second, they are pluripotent, and are capable to differentiate in cells and tissues of all three germ layers both *in vivo* and *in vitro*. In fact, the pluripotent nature of ESCs was demonstrated by their ability to contribute to all tissues of adult mice, including the germline, following their injection into host blastocysts⁷⁰. In addition to their developmental potential *in vivo*, ES cells show a notable capacity to form differentiated cell types *in vitro*^{71, 72}.

In order to maintain the pluripotency *in vitro*, it is crucial to prevent differentiation and to promote proliferation. Leukemia inhibitory factor (LIF) is one of the required extrinsic growth factors, that plays a central role in the maintenance of ESCs. These extrinsic factors are able to regulate and activate a network of key transcription factors that controls pluripotency. This network includes the homeodomain transcription factor Oct3/4⁷³, the variant homeodomain transcription factor Nanog⁷⁴ and the high mobility group (HMG)-box transcription factor Sox2⁷⁵.

All pluripotent cells, during mouse embryogenesis, in mouse embryonic stem cells and in embryonic germ cell lines express the POU transcription factor Oct (octamer-binding transcription factor) 3/4. Oct 3/4 deficient mouse embryos fail to form the inner cell mass, lose pluripotency and differentiate into trophectoderm⁷⁶.

Sox2 is expressed both in the ESCs and in neural stem cells, it is a member of the HMG-domain DNA-binding-protein family and it is implicated in the regulation of transcription and chromatin architecture ⁷⁷.

Finally, several studies confirm that the homeodomain transcription factor Nanog is a key factor to maintain pluripotency. It is known that Nanog can block primitive endoderm differentiation and neuronal differentiation ⁷⁸. Furthermore, nanog can inhibit mesodermal differentiation, interacting with Smad1, to inhibit the expression of Brachyury ⁷⁹.

When the factor that maintain the pluripotency in ESCs are removed, under appropriate conditions, they are able to differentiate and generate the three embryonic layers. Three general approaches are used to initiate ES cell differentiation.

In the first method, ES cells are allowed to aggregate and form three dimensional colonies also known as embryoid bodies (EBs) ^{72, 80}. In the second method, ES cells are cultured on stromal cells, and differentiation takes place in contact with these cells ⁸¹. The third protocol involves differentiating ES cells in a monolayer on extracellular matrix proteins ⁸².

Each of these approaches are able to differentiate ESCs and presents specific advantages and disadvantages. EBs provide a three-dimensional structure that enhances cell–cell interactions that may be important for certain developmental programs, on the other hand the complexity of the EBs can also be a disadvantage, because EBs generates cytokines and inducing factors that can complicate interpretations of experiments in which one is trying to understand the signaling pathways involved in lineage commitment. Moreover, EBs generation is generally performed in presence of retinoic acid ⁸³ that is a strong teratogen but perhaps, it is able to perturb neural patterning, inducing suppression of the forebrain development ^{84, 85}.

Co-culture with stromal cells provides the beneficial growth promoting effects of the particular cell line used. However, these supportive cells produce undefined factors that may influence the differentiation of the ES cells to undesired cell

types. An additional problem is the difficulty to separate the ES-cell-derived cells from the stromal cells.

Other protocols have been developed to differentiate ESCc into neurons, *in vitro*⁸⁶⁻⁸⁸. However, these procedures require extended *in vitro* culture⁸⁸ or results in low efficiency of neural induction^{86, 87}.

Recently, efficient neuronal differentiation has been performed in serum-free conditions. However, this method requires both EBs formation and inducing factors^{89, 90}. Parisi and collaborators have recently defined a fast and simple method, namely, KSR-monolayer method, to generate neurons and different neuronal sub-types from mouse ESCs, in absence of inducing factors and EBs formation⁹¹.

The feeder-independent E14Tg2a ESCs are cultured with KRS (Knockout Serum Replacement) and plated at low density in the proper differentiation method. Under this conditions, at 7 days of differentiation, a group of cells show neuron-like morphology. This phenomenon was accompanied by the formation of a complex neurite network surrounding the colonies.

Furthermore, in this kind of culture a lower number of cells differentiates in astrocytes and only sporadically in oligodendrocytes, and this suggests that neuron formation is preferred, compared to the others neuroectodermal derivatives. Finally, KSR monolayer method allows to generate multiple neuronal subtypes able to produce different neurotransmitters, and this important feature could be useful to investigate specific neurodegenerative diseases or to screen molecules that impair or improve neuronal differentiation.

Neuroblastoma SH-SY5Y cell line has generally been chosen as an experimental model for neuronal differentiation in order to study pathogenesis of degeneration and for drug screening. Being derived from neuroblastoma, SH-SY5Y cells are often induced to differentiate into neurons by different agents, such as retinoic acid (RA)⁹².

Neuronal differentiation induced by RA occurs with dopaminergic-like morphology, formation of neurites, whose length increases with time of

exposure, synthesis of neurospecific enzymes, neurotransmitters, neurofilaments formation and electrophysiologic modifications as seen in normal neurons.

RA treatment arrests cells at G1-phase of the cell cycle, inhibit DNA synthesis and growth already at 48 hours ⁹³.

1.4.2 *Caenorhabditis elegans* as an animal model

Caenorhabditis elegans is a nematode of ~1 mm at the adult stage, that can be found in the soil all over the world. It is widely used as a model organism in molecular research for several reasons:

- It has a small organization with a very simple anatomical structure.
- It is transparent and this facilitates observation of biological structures and processes using optical microscopy.
- It has a life cycle, which is completed in about 3 days, during which the worm passes through four larval stages. This very short life cycle allows to obtain, in a limited time, a large number of worms to study and analyze.
- It has two sexes, male and hermaphrodite. This allows the genetic analysis of its biology.
- It grows easily in the laboratory both on solid ground and in liquid medium, feeding bacteria (e.g. *Escherichia coli*). Fertile nematodes can be recovered after freezing (-80 ° C/-170 ° C), which facilitates the conservation of collections of mutant strains.
- Its genomic sequence is fully available.
- In addition to direct genetic approaches, *C. elegans* offers the possibility to use a wide range of reverse genetics methods for studying the function of genes of known sequence. A particularly important example is the use of interference with double-stranded RNA.

- It provides the opportunity to study *in vivo* the pattern of expression of a gene, using reporter genes or to study the function of specific protein domains via the generation of transgenic strains.

Its nervous system, relatively simple, is formed by 302 neurons, identified and described for position, shape, connections and synapses.

The complete sequence of the genome has documented the great conservation of gene sequences between nematodes and mammals, so that *C. elegans* has been used as a model to study the function and the role of certain genes in the molecular mechanisms involved in the pathogenesis of various human diseases. Indeed, *C. elegans* has been used as a model to study certain neurodegenerative diseases such as Parkinson's, ⁹⁴ Alzheimer's ⁹⁵ and other diseases by accumulation of toxic proteins such as those by polyglutamine expansion (e.g. Huntington's disease) ⁹⁵.

1.4.3 *C. elegans* and the oxygen deprivation response

The nematode *C. elegans* is emerging as an excellent model organism to study how animals are able to adapt and survive oxygen deprivation. In fact, the worm responds in qualitatively different ways, under the conditions of hypoxia or anoxia.

C. elegans can adapt to a " sublethal hypoxia (0.5% oxygen at 20 ° -22 ° C) activating or repressing genes controlled by the hypoxia-inducible transcription factor (HIF-1 α) ⁹⁶.

Several recent papers have described new roles for *C. elegans* HIF-1 and its interactors not only in stress responses but also in aging ⁹⁷⁻¹⁰¹. Indeed, many of the genes activated by HIF-1 have predicted roles in signal transduction or in the regulation of gene expression, and this suggests that HIF-1 initiates cascades of events that can increase stress resistance and promote longevity. It is known that some of the genes downstream of HIF-1 contribute to the formation of stress-resistant *dauer* state, that is a larval, arrested developmental variant of *C. elegans* that forms at the second molt in response to environmental stresses. Hif-1-deficient animals exhibit an increased frequency

of dauer formation at high temperatures ¹⁰². Finally in 2008, Pocock and Hobert demonstrate that low oxygen levels cause cell-specific defects in the *C. elegans* nervous system, in particular increasing the frequency of some axonal pathfinding aberrations stabilizing HIF-1 in neurons and muscle. Furthermore, nervous system defects occur also when reactive oxygen species (ROS) stabilize HIF-1 during hypoxia ¹⁰³.

The nematode *C. elegans* can survive the complete loss of oxygen (anoxia at 20 ° - 22 ° C) for at least one day in standard culture conditions, by entering a state of reversible arrest, called "suspended animation". Wild-type larvae and adults stop moving, eating, or laying eggs. Singularly, *C. elegans* can recover from 24 hours of anoxia-induced arrest and continue development. It has been shown that, in these conditions, several spindle elements, such as *san-1*, *mdf-2* and *bub-3*, are implicated in the anoxia-induced metaphase arrest ¹⁰⁴⁻¹⁰⁷. This involvement is crucial for embryonic survival and it is *hif-1* independent. At 0.1% oxygen, *C. elegans* arrests oocyte production and induces embryonic diapause in their embryos *in utero*. Also this process results *hif-1* independent ¹⁰⁸.

Finally, challenge to long-term anoxia (48-72 hours) or hypoxia at high temperatures (<0.3% oxygen at 26-28 ° C) is lethal for the worm, although recent studies have identified genes and pathways that increase the ability of the worms to survive under these extreme conditions. Animals that have been incubated at high temperatures in severe hypoxia or anoxia for more than 20 hours undergo pathologies in multiple tissues, including muscle, the nervous system, and the pharynx ^{104, 109, 110}.

1.4.4 *C. elegans* carbonic anhydrases

The genome of the nematode *Caenorhabditis elegans* encodes for six α CA isoforms (*cah-1*, 2, 3, 4, 5 and 6) ¹¹¹.

In literature it is known that one of these genes, *cah-4*, is regulated by both oxygen levels ¹¹² and environmental pH ¹¹³. Furthermore, using a worm model of muscular dystrophy, it was demonstrated that *cah-4* may also be involved in

the progression of muscle degeneration ¹¹⁴. *cah-4* has two splicing variants, *cah-4a* and *cah-4b*.

Amino acid sequence analysis revealed that the CAs of the nematode show a high homology to mammalian α class isoforms and that CAH-3, CAH-4 and CAH-5 present in their sequence three histidines that act as zinc ligands, as well as human CA II.

Fasseas and collaborators found that during the development each gene follows a unique expression pattern, indeed *cah-3* and *cah-4* are more expressed during L1 and L3 stages, whereas *cah-1*, *cah-2*, *cah-5* and *cah-6* show a less transcript accumulation ¹¹¹.

Interestingly, the *C. elegans* CAs can be clustered into two distinct groups that include: soluble isozymes, and acatalytic isozymes. CAH-1, CAH-2, and CAH-6 are acatalytic isozymes, indeed they miss certain residues necessary for catalytic activity. CAH-3 and CAH-5 are most closely associated with the soluble, catalytic human isozymes, while CAH-4 is related to the catalytic isozymes.

Experiments in which GFP expression is driven by CA promoters revealed that all nematode carbonic anhydrase are expressed in neurons (Figure 12). In general, only subsets of the 302 adult neurons expressed GFP, but it was found that CAH-6 and CAH-4a are expressed throughout the entire nervous system. Moreover, in addition to neuronal labeling, CAH-2a, CAH-3, and CAH-5 were strongly expressed in the intestine, CAH-4b and CAH-5 in the hypodermis, CAH-2a, CAH-3, CAH-4a, CAH-4b, and CAH-5 in various muscle cells including the vulva and pharynx.

These experiments elucidated nematode CAs subcellular distribution. In particular, CAH-3, CAH-4b, and CAH-5, that were predicted to be catalytic, were found in the cytoplasm. CAH-1 and CAH-2, two of the putative acatalytic isozymes, were intracellular, but punctate. CAH-4a was also observed in the nuclear compartment ¹¹⁵. This last observation was unforeseen, and further

investigations revealed that, in the first exon of *cah-4* there is a sequence encoding for a putative NLS ¹¹⁵.

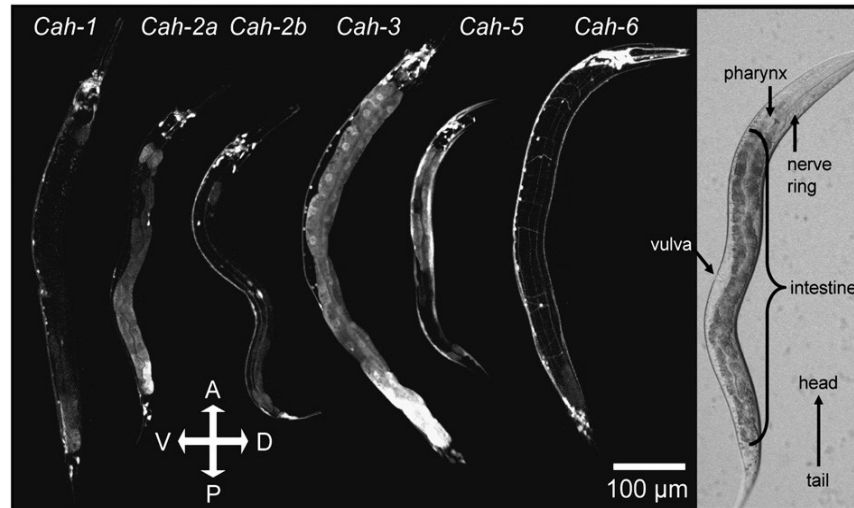


Figure 12. *Cah* gene expression patterns. Representative confocal image of L4 worms in which GFP expression is driven by a specific *cah* promoter ¹¹⁵.

2. AIMS OF THE THESIS PROJECT

Hypoxia is a state of oxygen deficiency, in tissues and cells, sufficient to impair functions of the brain and other organs. A consequence of this deprivation is a decrease of the intracellular pH of neurons and glial cells. The maintenance of an adequate pH is a key factor in the functioning of the Central Nervous System (CSN). It is important to better understand the pathways involved in the response to hypoxia and the processes that occur in mature neurons, in order to find possible players that can prevent neurodegeneration and trigger cell survival pathways.

In a recent paper, I contributed to the characterization of the interactome of CA IX³⁴. An unexpected, although exciting result emanating from such study did reveal CA IX as a nuclear protein in mammalian cell lines. Based on these results, I undertook functional analysis of CA IX and selected members of its interactome in neuronal cellular models. The first selected model is represented by a widely used human neuroblastoma cell line, SH-SY5Y, able to differentiate into dopaminergic-like neurons after treatment with retinoic acid. The second one corresponds to mouse ES pluripotent cells induced to differentiate to multiple neuronal subtype. Indeed, I evaluated subcellular distribution of CA IX in both models, and I revealed the putative sequences involved in its nuclear trafficking. Taking advantage of the neuroblastoma model, I also evaluated functional interaction of CA IX with CAND1, and provided the first evidence for a nuclear function of CA IX.

Finally, I performed a preliminary characterization of two carbonic anhydrases of the nematode *C. elegans*, in order to study carbonic anhydrases function in a animal model, taking advantage of such *in vivo* system.

3. RESULTS

3.1 Characterization of CA IX interactome

In order to characterize the interactome of CA IX, I selected a biochemical approach. For production of the biochemical bait, a DNA sequence encoding a C-terminal Strep-tag was fused to the full-length human CA IX cDNA; the corresponding construct was then transfected into HEK-293 cells line, due to the high transfection efficiency of these cells. The transfected cells were cultured both in normoxic and hypoxic conditions.

To capture possible interactors of CA IX, the CA IX Strep-tag protein from the transfected cells was co-purified with the bound proteins on a Strep-tactin column. The co-purified proteins, from normoxic and hypoxic cells, were separated by SDS-PAGE and revealed by silver nitrate staining (Figure 13). After staining, in order to identify the bound proteins, each gel lane was cut in 21 slices and analyzed by nLC-ESI-LIT-MS/MS for protein identifications (Table 1). The analysis of the identified proteins showed a higher number of specific proteins in the hypoxic condition, compared to the few proteins found in the normoxic condition. The latter group includes the mitochondrial ATP synthase α/β subunits (ATP5A1 and ATP5B) and Ras GTPase-activating protein-binding protein 2 (G3BP2), a scaffold protein involved in the mRNA transport; also ribosomal protein RPS5, the catalytic subunit of the tRNAsplicing ligase complex UPF0027, and CAND1 (cullin-associated NEDD8-dissociated protein 1) were identified among the potential CA IX interactors under normoxia. These last members were also captured in hypoxic cells. The interactome specific for the hypoxic condition, together with the acetyl-CoA carboxylase 1 enzyme (ACACA), the HEAT repeat-containing protein 3 (HEATR3), the mitochondrial trifunctional enzyme subunit alpha (HADHA), the protein SAAL1, and CAND2 (cullin-associated NEDD8-dissociated protein 2), comprises a series of proteins belong to the nucleo-cytoplasmic transport machinery.

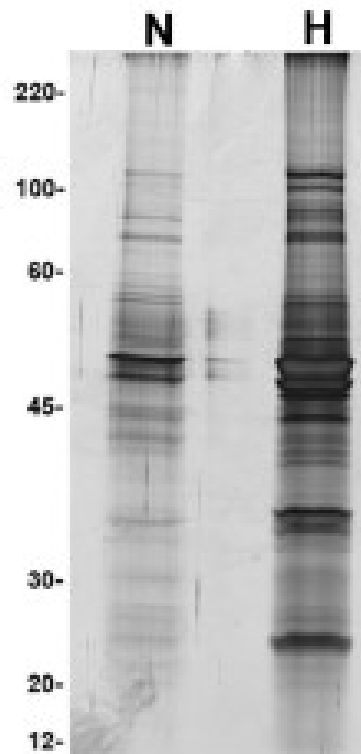


Figure 13. SDS-PAGE analysis of the CA IX interacting proteins in HEK-293 cells. Proteins extracted from normoxic (N) and hypoxic (H) cells transfected with the Strep-tag CA IX vector were loaded on Strep-Tactin columns for co-purification of CA IX and its binding partners. Eluates were separated on a 10% SDS-PAGE gel and detected by silver nitrate staining. After staining, each lane was cut into 21 slices to identify proteins by nLC-ESI-LIT-MS/MS analysis

34

The identified proteins were analyzed by the database STRING in order to understand the physical and/or predicted functional relationships between them (Figure 14). STRING analysis did indeed highlight a large network, including most of the identified proteins; they were related to the nucleo-cytoplasmic transport, such as importin- α (KPNA2), importin- β (IPO4, IPO5, IPO7, IPO9, TNPO1, TNPO3) and exportins (XPO1, XPO2/CSE1L, XPO5, XPOT). After

STRING analysis, the potential CA IX interactors were classified under gene ontology parameters (namely, biological process and INTERPRO) in the DAVID bioinformatic database. The platform DAVID confirms the cluster defined by STRING database. In addition, the DAVID platform highlights a less obvious group of 13 out of the 25 identified proteins, characterized by ARM and HEAT repeats. Among these proteins are included most of the members involved in the nucleo-cytoplasmic transport machinery, and additional proteins, such as CAND1, CAND2 and HEATR3.

Accessi	Description	Normoxi	Hypox
Q16790	Carbonic anhydrase 9, CA9 [CAH9_HUMAN]	X (bait)	X
Q13085	Acetyl-CoA carboxylase 1, ACACA [ACACA_HUMAN]		X
Q9UBB4	Ataxin-10, ATXN10 [ATXN10_HUMAN]		X
P25705	ATP synthase subunit alpha, mitochondrial, ATP5A1 [ATPA_HUMAN]	X	
P06576	ATP synthase subunit beta, mitochondrial, ATP5B [ATPB_HUMAN]	X	
P00918	Carbonic anhydrase 2, CA2 [CAH2_HUMAN]		X
Q86VP6	Cullin-associated NEDD8-dissociated protein 1, CAND1 [CAND1_HUMAN]	X	X
O75155	Cullin-associated NEDD8-dissociated protein 2, CAND2 [CAND2_HUMAN]		X
O14980	Exportin-1, XPO1 [XPO1_HUMAN]		X
P55060	Exportin-2, CSE1L [XPO2_HUMAN]		X
Q9HAV4	Exportin-5, XPO5 [XPO5_HUMAN]		X
O43592	Exportin-T, XPOT [XPOT_HUMAN]		X
Q7Z492	HEAT repeat-containing protein 3, HEATR3 [HEATR3_HUMAN]		X
P52292	Importin subunit alpha-2, KPNA2 [IMA2_HUMAN]		X
Q8TEX9	Importin-4, IPO4 [IPO4_HUMAN]		X
O00410	Importin-5, IPO5 [IPO5_HUMAN]		X
O95373	Importin-7, IPO7 [IPO7_HUMAN]		X
Q96P70	Importin-9, IPO9 [IPO9_HUMAN]		X
Q96ER3	Protein SAAL1, SAAL1 [SAAL1_HUMAN]		X
Q9UN86	Ras GTPase-activating protein-binding protein 2, G3BP2 [G3BP2_HUMAN]	X	
Q9Y5M8	Signal recognition particle receptor subunit beta, SRPRB [SRPRB_HUMAN]		X
Q92973	Transportin-1, TNPO1 [TNPO1_HUMAN]		X
Q9Y5L0	Transportin-3, TNPO3 [TNPO3_HUMAN]		X
P40939	Trifunctional enzyme subunit alpha, HADHA [ECHA_HUMAN]		X
Q9Y310	UPF0027 protein C22orf28, C22orf28 [CV028_HUMAN]	X	X
P46782	40S ribosomal protein S5, RPS5 [RS5_HUMAN]	X	X

Table 1. List of potential interactors of CA IX identified under Normoxic and Hypoxic conditions

The experiments aiming to characterize the interactome for CA IX were performed in HEK293 cells, taking advantage of an overexpression system, in which the CA IX protein was fused to an artificial Strep-tag. On the other hand, the obtained results clearly indicated that CA IX, despite its membrane topology, did behave similarly to a protein subjected to nuclear import and export. The subcellular localization of CA IX was then evaluated in human cell lines of different origin by confocal immunofluorescence analysis (Figure 15). In agreement with data present in literature, regarding the high expression levels of CA IX in high density cell cultures, the GEO cell line, derived from a colorectal carcinoma, showed a strong expression of CA IX at the level of the cell membrane. To this location is also associated, in some cells, weak staining at the nuclear and perinuclear regions. On the contrary, the remaining cell lines, including HEK-293 (kidney carcinoma), SHSY5Y (neuroblastoma) and BJ5ta (immortalized fibroblasts) showed a wider distribution of CA IX with extreme decrease in membrane staining and strong accumulation at the nuclear level. These data clearly support the interactome data, showing that CA IX may possess prevalent membrane localization in some cells, as well as a complex subcellular localization in most mammalian cells, including the SH-SY5Y neuroblastoma cell line (Figure 14)³⁴. These cells are indeed able to differentiate in response to a differentiating agent, such as all-*trans*-retinoic acid (RA)¹¹⁶. These data encouraged me to further investigate the functional significance of nuclear CA IX and of its interactome in cellular models of neuronal differentiation, including the SH-SY5Y cells and murine embryo stem cells (ES).

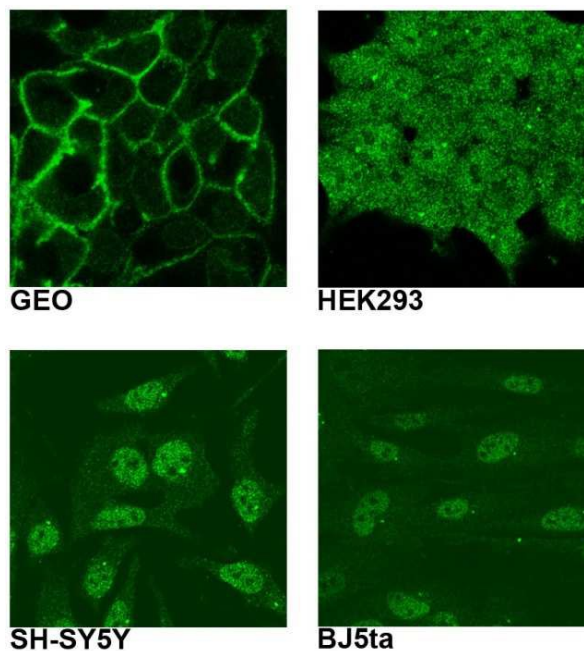


Figure 15. Subcellular distribution of CA IX in human cell lines. GEO (colon adenocarcinoma), HEK-293 (embryonic kidney carcinoma), SH-SY5Y (neuroblastoma) and BJ5T α (telomerase immortalized fibroblasts) cells were fixed and permeabilized to detect CA IX (green). In GEO cells, CA IX is localized in plasma membrane, whereas in the other cell lines it is broadly distributed, with a positive staining of nuclei.

3.2 CA IX expression and subcellular distribution in cellular models of neuronal differentiation

SH-SY5Y cells are able to differentiate, *in vitro*, into dopaminergic-like neurons, if stimulated with differentiating agents ¹¹⁶. In order to evaluate the potential role of CA IX as a pro-survival factor, I evaluated protein expression in differentiated cells. After three days of treatment, retinoic acid (RA)-differentiated and undifferentiated SH-SY5Y cells were cultured in both normoxic and hypoxic conditions. A western blot analysis was performed to appraise the expression of CA IX and its interactors (Figure 16). In normoxic and hypoxic conditions,

CAND1 and XPO1 present an equal amount of expression both in undifferentiated and in differentiated cells. Interestingly, the basal expression of CA IX protein in normoxia was increased in differentiated cells, compared to control cells. This difference in expression was also occurring, and even more pronounced, in hypoxic cells. β 3-tubulin expression was evaluated as differentiation marker in the western blot experiment, while β -actin was used as a loading control.

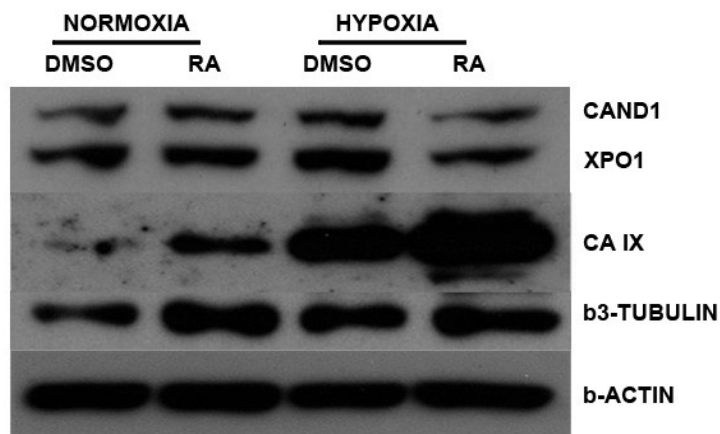


Figure 16. CA IX and its interactors in undifferentiated and differentiated SHSY5Y cell line. CA IX expression in differentiated cells is higher than in undifferentiated cells, both in normoxic. and in hypoxic condition. CA IX interactors, CAND1 and XPO1, present an equal amount both in undifferentiated and in differentiated cells. β 3-Tubulin was used as differentiation marker and it was more expressed in the treated cells, while β -actin was used as a loading control.

To confirm these data and to evaluate subcellular localization of CA IX in differentiated cells, I performed a confocal immunofluorescence analysis. The images show that in undifferentiated cells (bottom panel on the left in figure 17) CA IX is expressed in the cytoplasm and it is abundant in the nucleus too. In differentiated cells nuclear representation of CA IX is prominent, in comparison to their undifferentiated counterpart. So, these data are in agreement with the western blot data; furthermore, they clearly show nuclear enrichments of CA IX in differentiated cells.

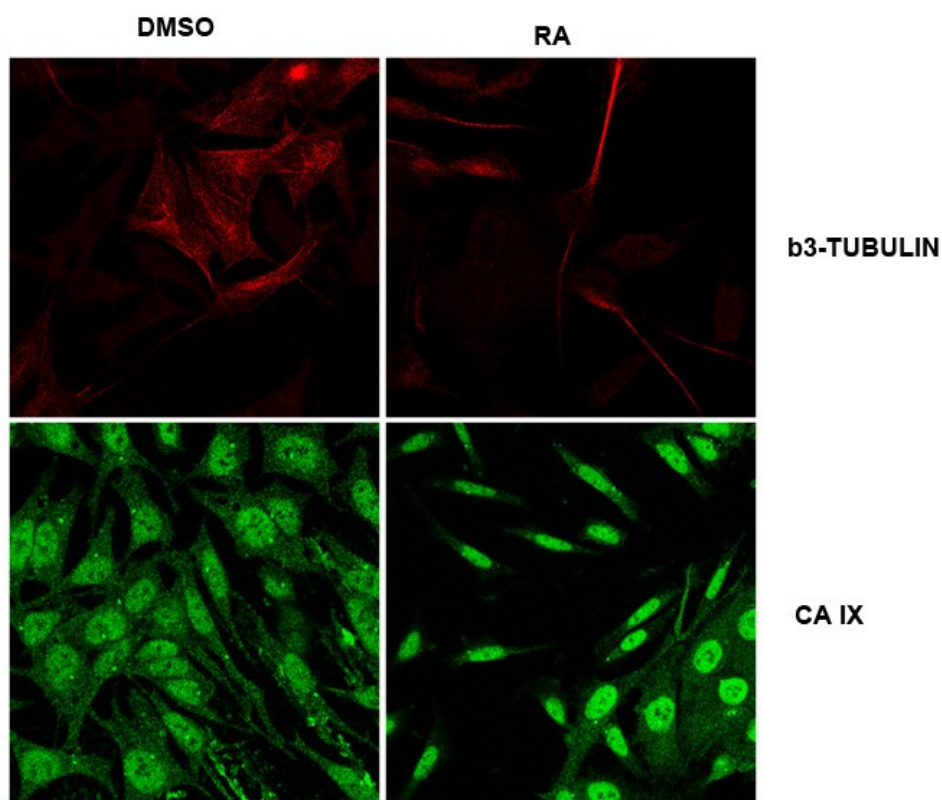


Figure 17. Subcellular distribution of CA IX in undifferentiated and differentiated SHSY5Y cell line. CA IX is expressed in the cytoplasm, but it is much more abundant in the nucleus, compared to their undifferentiated counterpart. β 3-tubulin is a differentiation marker and it is abundant in the neurofilaments of differentiated cells.

Western blot and immunofluorescence analysis were performed in murine embryonic stem cells too. This analysis did indeed reveal that CA IX was not expressed in undifferentiated embryonic stem cells (first lane, Figure 18).

In cells induced to differentiate into neurons, at 5-days timepoint, when in the culture plate are present neuronal progenitor cells, CA IX expression is still not detectable (second lane), whereas it can be appreciated at 12 days, when the progenitors differentiate completely into neurons and glial cells (third lane).

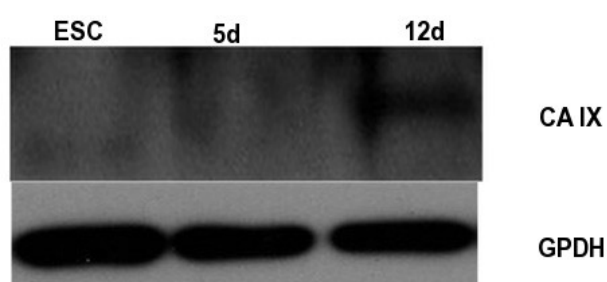


Figura 18. CA IX expression in murine stem cells. CA IX is not expressed in embryonic stem cells and In cells induced to differentiate into neurons (5 days), but it is expressed at 12days.

In order to evaluate CA IX subcellular expression in embryonic stem cells and in differentiated cells, I performed an immunofluorescence analysis (Figure 19).

Confirming biochemical data, these experiments revealed that CA IX (green) was not expressed in embryonic stem cells, that are indeed positive for OCT 3/4 (red), a stem cell marker; CA IX expression was still not detectable at 4 days of differentiation, when cells were positive for SOX 1 (red), a neural progenitors marker.

At 7 days of differentiation, there was a group of cells stained for CA IX (green) in the nucleus, but not for SOX 1 (red) too, and another group stained only for this marker; to assess whether the cells that express the nuclear CA IX are neuronal cells, I used β 3-tubulin, that is a marker for post-mitotic neurons. The three panels of figure 19 show that several cells were both CA IX (green) and β 3-tubulin positive (red), and that CA IX was abundantly expressed in the nuclei of this subpopulation of neurons.

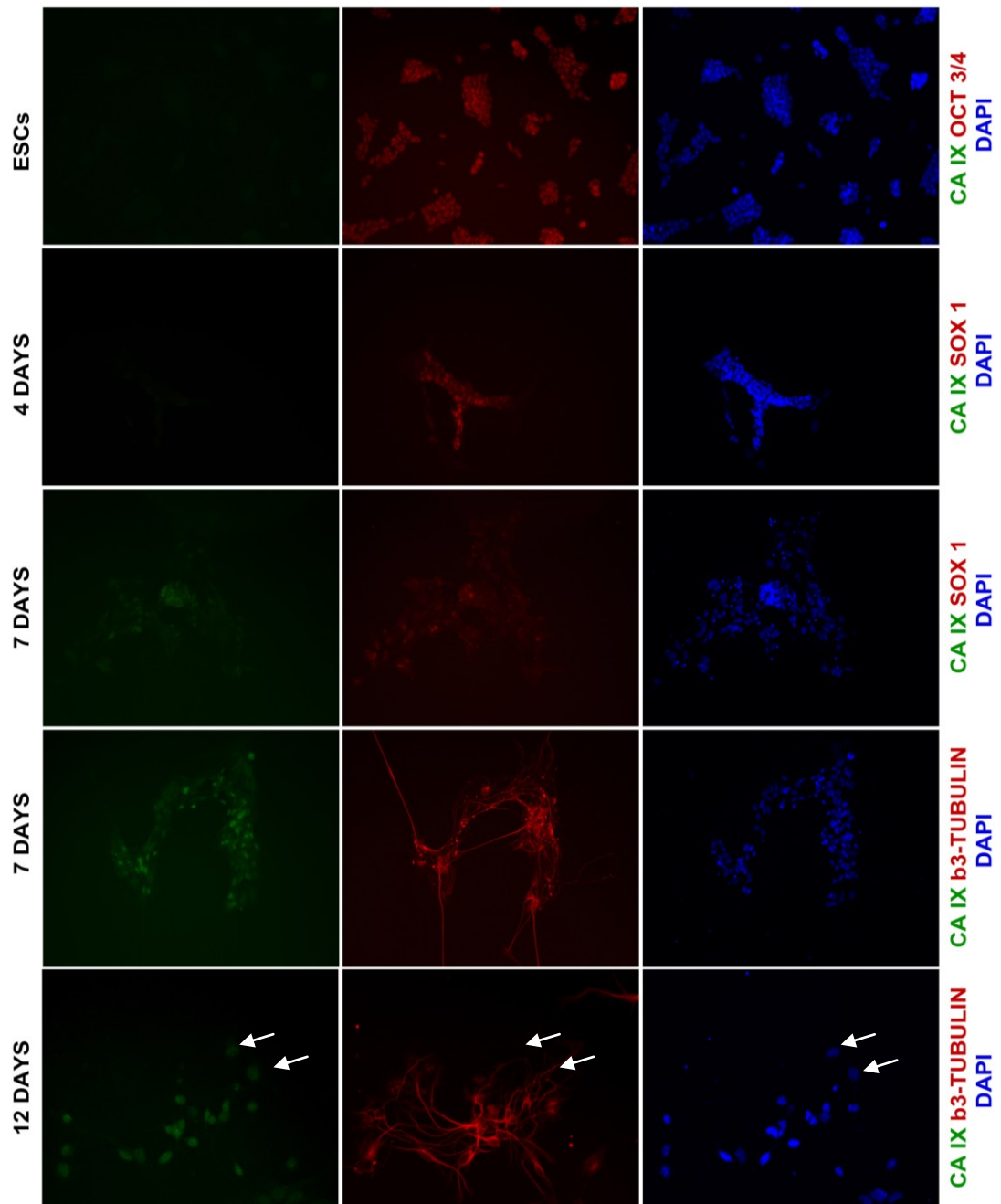


Figure 19. CA IX expression in ESCs and differentiated ESCs. CA IX (green) expression is not detectable in ESCs and in 4-days differentiated ESCs. At 7 days a group of cells are stained for CA IX in the nucleus, but not for SOX1 (red). At the same time point, another group of cells are positive for both CA IX and β3-tubulin (red). At 12 days of differentiation, the nuclear CA IX expression was still evident in neuronal cells, but also β3-tubulin negative cells. Nuclei are highlighted by DAPI staining (blue).

Finally, even at 12 days of differentiation, the nuclear CA IX expression was still evident in neuronal cells, but also in β 3-tubulin negative cells (bottom left panel, indicated by white arrows). Further investigations will be required to identify the nature of this last group of cells.

In all the experiments, nuclei were highlighted by DAPI (blue).

Altogether, these results support the existence of a nuclear pool for CA IX, both in human differentiated and undifferentiated cells (SH-SY5Y) and in mouse cells, but for this last group, its expression was restricted to differentiated cells.

3.3 Analysis of putative nuclear localization and nuclear export signals in the CA IX sequence

Although CA IX is known as a transmembrane protein, our evidences define it as a nuclear protein in a variety of human cells. More interestingly, nuclear representation of CA IX is induced in hypoxic cells and is a prominent feature in two different models of neuronal differentiation.

Interactome analysis revealed that CA IX interactors are mainly intracellular proteins; this occurrence was also confirmed by the identification of the cytosolic tail of CA IX as the actual binding site for its interactors. Using bioinformatic analysis on the CA IX protein sequence, I identified a hydrophobic region, which might act as nuclear export signal (NES) for interaction with exportin, being rich in leucine, and a basic region, similar to a nuclear localization signal (NLS), in the C-terminal region. Two softwares were used to analyze CA IX sequence: NetNES and NLStradamus. The software NetNES suggests that the sequence ILALVFGL is a putative NES (415-422), and the NLStradamus one indicates the sequence RRGHRRGTKGG as a putative NLS (436-446) (Figure 20).

To assess whether the basic and the hydrophobic regions identified in CA IX can actually perform as NLS or NES, respectively, I evaluated whether they were able to drive the subcellular distribution of a reporter protein. To this aim,

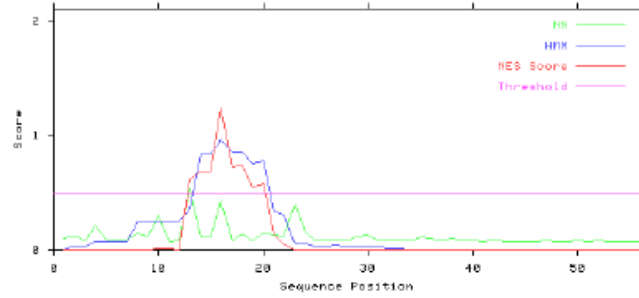
several fusion constructs in which GFP was in-frame fused at the C-terminus with canonical and CA IX putative NES and or NLS sequences, were generated to be transfected in SH-SY5Y cells and analysed by confocal fluorescence microscopy (Figure 21). The patterns of subcellular distribution of the GFP fusions obtained from each CA IX construct were compared to the localizations of the corresponding proteins with the canonical signals, as well as to the pattern of the isolated GFP.

Cells expressing only GFP showed a strong signal, which was equally distributed within cytoplasm and nucleus; the GFP_putative CA IX NLS localized predominantly in the nucleus, to a similar extent, compared to the canonical NLS signal. Nuclear localization of the reporter proteins was indeed confirmed by DRAQ5 staining (Figure 22).

Adding a NES signal to the NLS canonical sequence clearly moves back to the cytoplasm the new protein encoded by the GFP_canonical NES+NLS construct. This happens in a even more pronounced occurrence in the cells expressing the GFP protein, fused to both putative NES and NLS sequences from CA IX (GFP_putative CA IX NES+NLS construct) (Figure 23).

>Sequence - NetNES 1.1 prediction

NetNES 1.1: Predicted NES signals in Sequence



#Seq-Pos-Residue	ANN	HMM	NES	Predicted
Sequence-1-P	0.097	0.000	0.000	-
Sequence-2-V	0.115	0.028	0.000	-
Sequence-3-Q	0.078	0.028	0.000	-
Sequence-4-L	0.208	0.071	0.000	-
Sequence-5-N	0.085	0.071	0.000	-
Sequence-6-S	0.089	0.071	0.000	-
Sequence-7-C	0.090	0.071	0.000	-
Sequence-8-L	0.141	0.248	0.000	-
Sequence-9-A	0.115	0.244	0.000	-
Sequence-10-A	0.301	0.244	0.008	-
Sequence-11-G	0.071	0.244	0.006	-
Sequence-12-D	0.076	0.244	0.003	-
Sequence-13-I	0.535	0.356	0.615	Yes
Sequence-14-L	0.105	0.837	0.688	Yes
Sequence-15-A	0.109	0.837	0.687	Yes
Sequence-16-L	0.426	0.959	1.235	Yes
Sequence-17-V	0.084	0.850	0.728	Yes
Sequence-18-F	0.135	0.851	0.740	Yes
Sequence-19-G	0.084	0.756	0.545	Yes
Sequence-20-L	0.152	0.773	0.570	Yes
Sequence-21-L	0.131	0.336	0.138	-
Sequence-22-F	0.122	0.306	0.048	-
Sequence-23-A	0.399	0.051	0.000	-
Sequence-24-V	0.163	0.053	0.000	-
Sequence-25-T	0.078	0.028	0.000	-
Sequence-26-G	0.082	0.028	0.000	-
Sequence-27-V	0.082	0.036	0.000	-
Sequence-28-A	0.076	0.023	0.000	-
Sequence-29-F	0.116	0.023	0.000	-
Sequence-30-L	0.126	0.020	0.000	-
Sequence-31-V	0.076	0.016	0.000	-
Sequence-32-Q	0.085	0.015	0.000	-
Sequence-33-M	0.084	0.015	0.000	-
Sequence-34-R	0.079	0.000	0.000	-
Sequence-35-R	0.109	0.000	0.000	-
Sequence-36-Q	0.096	0.000	0.000	-
Sequence-37-H	0.084	0.000	0.000	-
Sequence-38-R	0.097	0.000	0.000	-
Sequence-39-R	0.082	0.000	0.000	-
Sequence-40-G	0.080	0.000	0.000	-
Sequence-41-T	0.074	0.000	0.000	-
Sequence-42-F	0.091	0.000	0.000	-
Sequence-43-G	0.073	0.000	0.000	-
Sequence-44-G	0.068	0.000	0.000	-
Sequence-45-V	0.070	0.000	0.000	-
Sequence-46-S	0.065	0.000	0.000	-
Sequence-47-Y	0.077	0.000	0.000	-
Sequence-48-R	0.072	0.000	0.000	-
Sequence-49-P	0.072	0.000	0.000	-
Sequence-50-A	0.075	0.000	0.000	-
Sequence-51-E	0.068	0.000	0.000	-
Sequence-52-V	0.075	0.000	0.000	-
Sequence-53-A	0.071	0.000	0.000	-
Sequence-54-E	0.073	0.000	0.000	-
Sequence-55-T	0.068	0.000	0.000	-
Sequence-56-G	0.073	0.000	0.000	-
Sequence-57-A	0.074	0.000	0.000	-

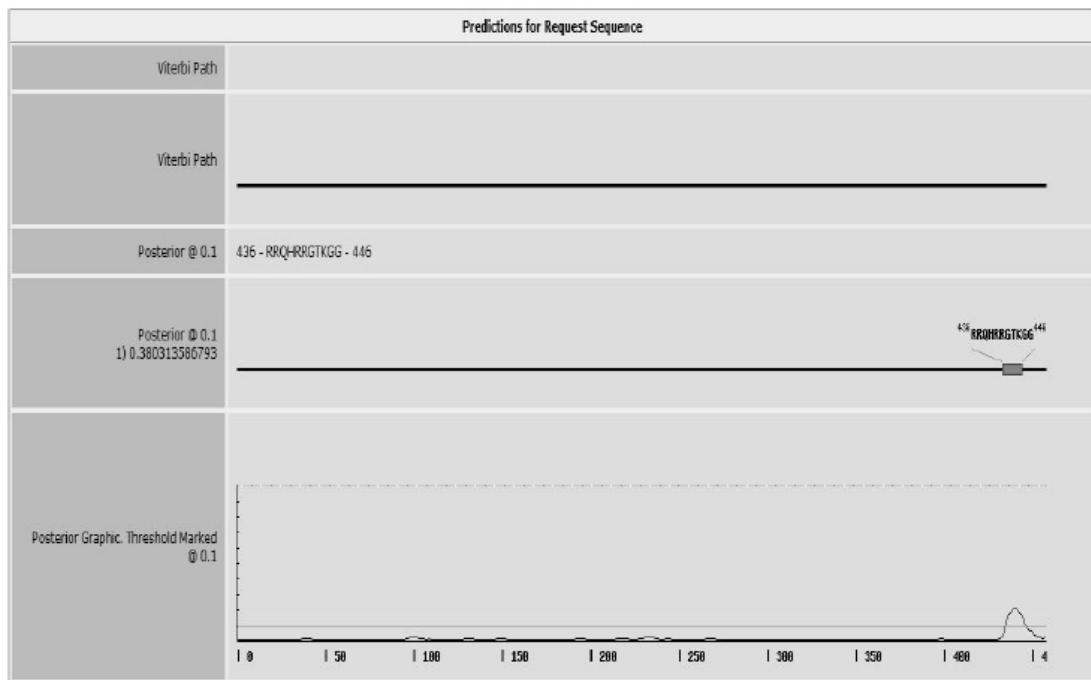


Figure 20. Bioinformatic analysis of CA IX (A) A putative NES sequence has been predicted by NetNES in the transmembrane region (<http://www.cbs.dtu.dk/services/NetNES/>); (B) A putative NLS sequence has been predicted by NLStradamus in the intracellular tail (<http://www.moseslab.csb.utoronto.ca/NLStradamus/>).

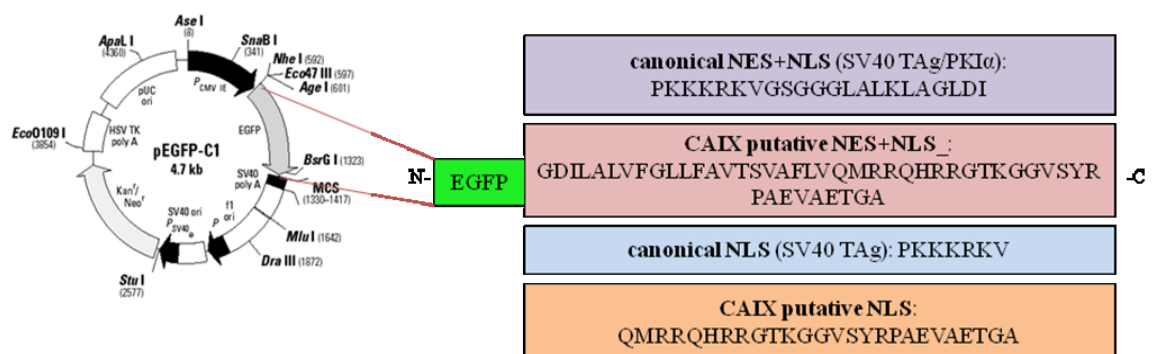


Figure 21. GFP Fusion constructs. GFP was in-frame fused at the C-terminus with the following sequences: canonical NES+NLS, CA IX putative NES+NLS, canonical NLS and CA IX putative NLS.

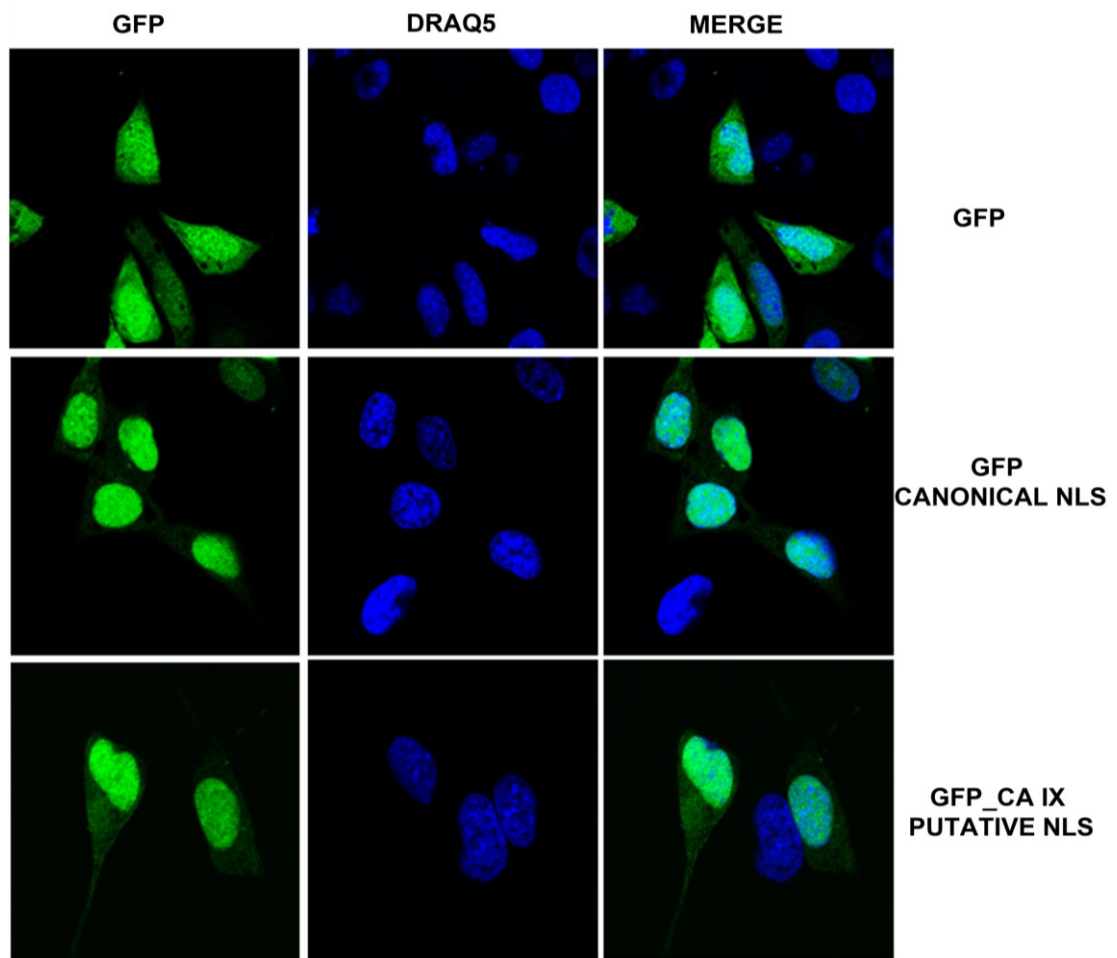


Figure 22. Subcellular localization of GFP-NLS fusion proteins. The nuclei of SHSY5Y cells transfected with GFP, GFP canonical NLS and GFP_CA IX putative NLS are highlighted with DRAQ5 staining (second column). The GFP is localized prevalently in the nucleus of all kind of cells, as shown in the first column and highlighted in the merge column.

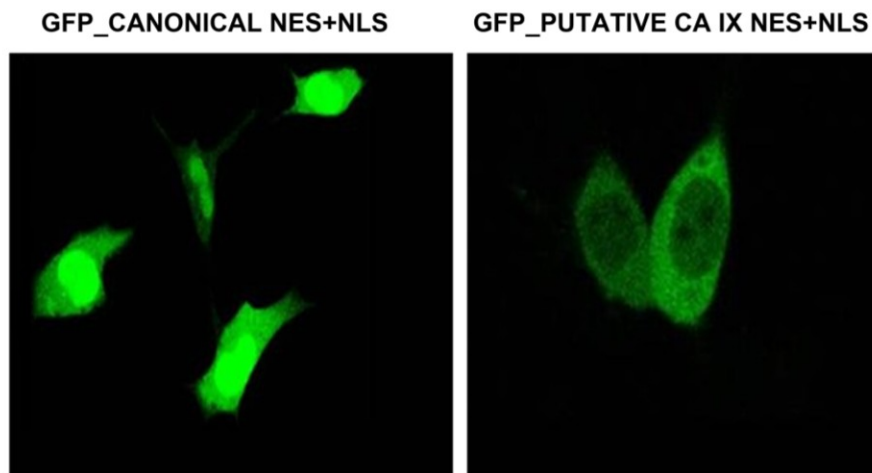


Figure 23. subcellular distribution of GFP_NES+NLS fusion protein. In cells transfected with the canonical signal, GFP is diffused inside the cells, but the nuclear signal is more marked than that of the cells that expressed the GFP alone (Figure 10R). In cells that expressed the CA IX putative signal GFP expression is higher in the cytoplasm than in the nucleus.

In conclusion, these data suggest that the putative NLS and NES sequences identified in the C-terminal tail of CA IX are actually able to direct a reporter protein to the nucleus (NLS), or to actively export it back to the cytosol (NES).

3.4 CA IX is bound to the chromatin of the 45S rRNA precursor

Immunofluorescence analysis indicated that CA IX had a nuclear localization, furthermore, the presence of the ribosomal protein RPS5, a protein involved in the assembly of ribosomes and in the maturation of ribosomal RNAs (rRNA), among the identified interactor of CA IX, strongly supports the participation of CA IX to ribosomal biogenesis. Finally, previous investigation showed CA IX co-localization with XPO1, in the nucleoli of HEK293 cells ³⁴.

In order to clarify a potential role of CA IX in ribosomal biogenesis, I performed a Chromatin-Immunoprecipitation assay (ChIP) in SH-SY5Y cells, grown under normoxic and hypoxic conditions, on the pre-rRNA 45S gene. The Upstream Binding Factor (UBF), that is a transcription factor required for expression of the 45S rRNA precursor ¹¹⁷ (from which 18S, 5.8S, and 28S ribosomal RNAs are generated), was used as a positive control for the ChIP assay.

In normoxic conditions (Figure 24), ChIP experiments with CA IX antibody showed a significant enrichment of CA IX on two different DNA fragments from the pre-rRNA 45S gene (blue bars). In hypoxic condition, the recruitment of CA IX on the pre-rRNA 45S gene was strongly decreased (red bars). Interestingly, the ChIP experiment carried out with the UBF antibody showed a perfect complementary pattern, in comparison to CA IX, since the interaction of UBF with the pre-rRNA 45S gene was stronger in hypoxia (red bars), compared to normoxia (blue bars).

These data strongly suggest that CA IX has a role on pre-rRNA 45S gene transcription, although it is not possible to establish whether CA IX does bind directly to DNA, or it does act in scaffolding complexes. This experiment, however, strongly supports a functional significance for nuclear presence of CA IX in SH-SY5Y cells.

In the same experiment I also investigated the presence of CA IX on this gene in undifferentiated and differentiated SH-SY5Y cells. A decrease of CA IX and UBF binding to the gene promoter can be observed in RA-differentiated cells

(green bars) compared to DMSO-undifferentiated ones (violet bars) (Figure 25).

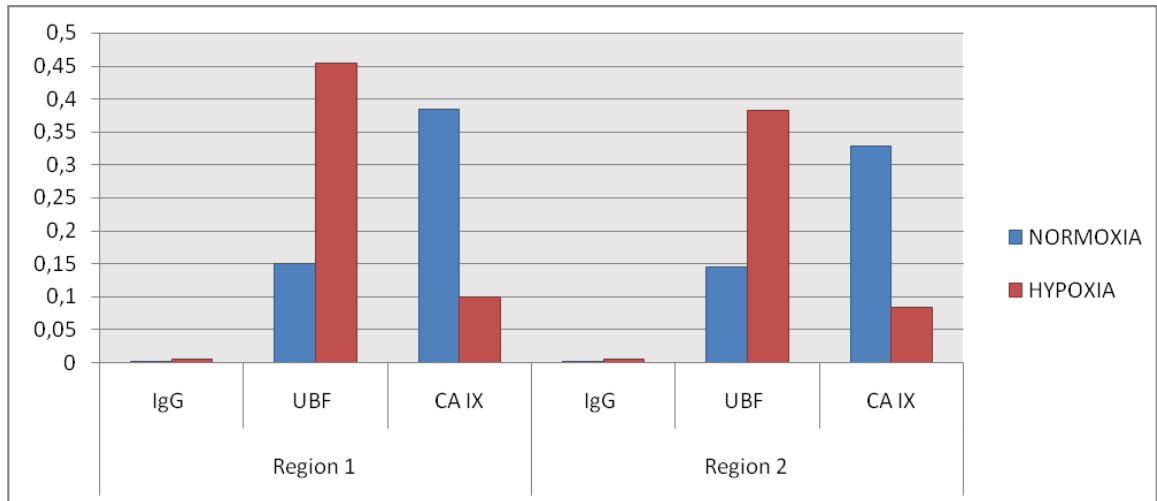


Figure 24. Chromatin-Immunoprecipitation assay rRNA 45S gene. In normoxic conditions, CA IX is present on the the pre-rRNA 45S gene, conversely in the hypoxic condition. UBF show a complementary trend.

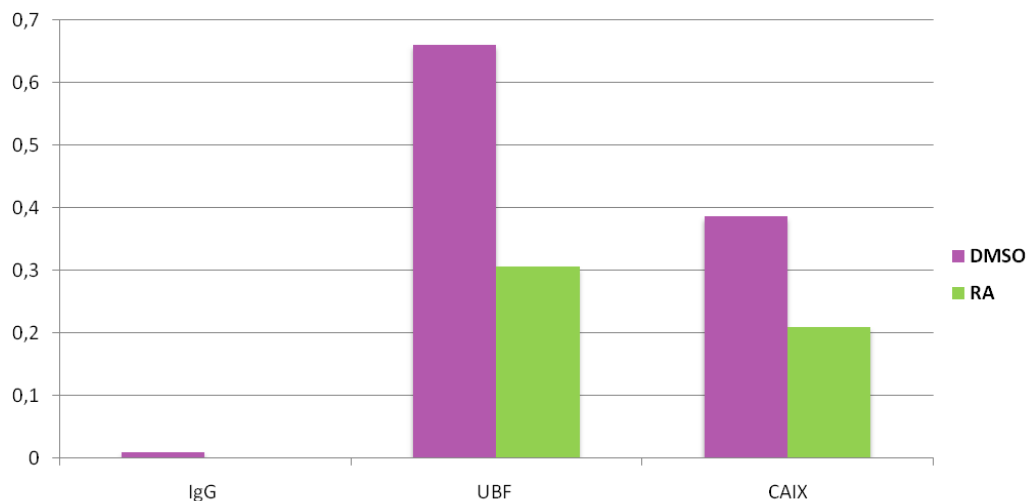


Figure 25. Chromatin-Immunoprecipitation assay of rRNA 45S gene in undifferentiated and differentiated cells. CA IX and UBF binding decreased in differentiated SH-SY5Y cells compared to the undifferentiated counterpart.

3.5 Functional validation of CA IX-CAND1 interaction

Among proteins identified as CA IX interactors rises a protein involved in important biological processes, including regulation of transcription and proteasome-mediated protein degradation, namely, CAND1¹¹⁷.

To confirm this identification and the real physical interaction of CAND1 with CA IX, co-precipitation experiments were performed in SH-SY5Y cells (Figure 26). Results validated this interaction. Indeed, the figure shows that CAND1 co-precipitated with CA IX under both normoxic and hypoxic conditions. In particular, the native complexes composed by both CAND1 and CA IX were most appreciable in hypoxia.

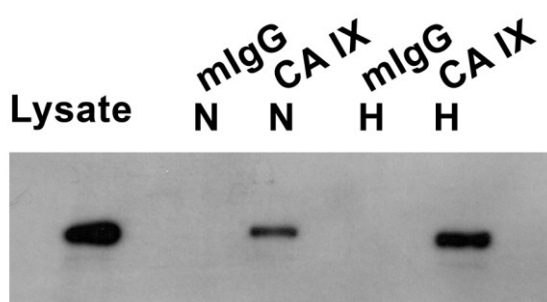


Figure 26. Analysis of endogenous CA IX/CAND1 protein complexes in normoxic and hypoxic SH-SY5Y cells. Immunoprecipitates from normoxic (lane 2 and 3) and hypoxic (lane 4 and 5) SHSY5Y cells were probed with CAND1 antibody. The extracts of lanes 2 and 4 were precipitated with control mouse IgGs, while the extracts of lines 3 and 5 were precipitated with CA IX VII/20 antibody. Input lysate was loaded in line 1

Based on these results, showing a physical interaction of CA IX with CAND1, I undertook the analysis of a possible functional interaction between the two proteins. To this aim, I generated SH-SY5Y cell clones expressing decreased levels of CAND1 protein through RNA interference. The most effective

construct, eliciting CAND1 down-regulation, namely, sh2555, was used for further experiments.

CAND1 protein is involved in regulation of protein stability through inhibition of assembly of SCF E3 ubiquitin ligase complex, that targets protein for degradation by 26S proteasome⁶⁷. Given that the CA IX/CAND1 complex was more abundantly represented in hypoxic cells, and CA IX is stabilized in hypoxia, we indeed evaluated whether CAND1 was actually involved in CA IX protein stabilization. Thus, I assessed the CA IX levels in cell lysates from sh2555.5 clone stably interfered with CAND1, by western blotting. Figure 27 shows the results of this analysis. As expected, both in normoxia and in hypoxia CAND1 is downregulated in sh2555.5 clone, compared to cells expressing a non silencing construct (shNS); the western blot clearly shows that CA IX is more abundantly expressed in hypoxic cells, compared to normoxic cells. The main result clearly showed that in both conditions, CA IX did result down-regulated in the sh2555.5 clone, compared to shNS; this actually occurred in both normoxia and hypoxia; interestingly, I also observed a parallel decrease in XPO1 protein levels in the clone interfered with CAND1 in comparison to control shNS cells. These results support the hypothesis that CA IX is indeed a target of the Ubiquitin-Proteasome Pathway (UPP), and that a functional interaction between CA IX and CAND1 does actually occur, possibly resulting in a higher stability of CA IX protein.

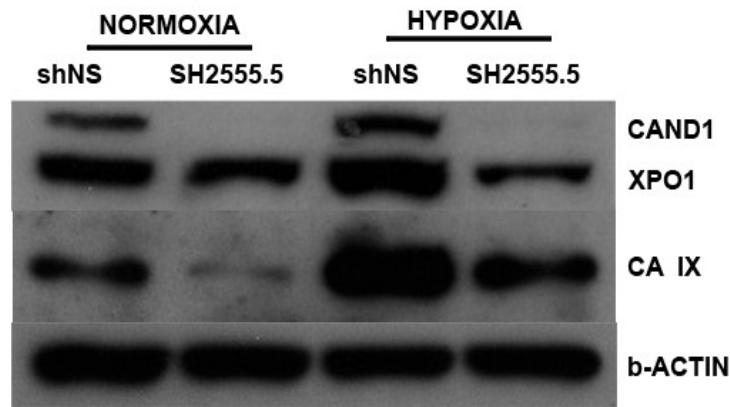


Figure 27. CA IX and its interactors in SHSY5Y cell clone expressing decreased levels of CAND1. Both in normoxia and in hypoxia CAND1 is downregulated in sh2555.5 clone, compared to shNS clone. CA IX did result down-regulated in the sh2555.5 clone, compared to shNS, in both normoxia and hypoxia; parallel decrease in XPO1 protein levels in the clone interfered with CAND1 in comparison to control shNS cells was observed too. β -actin was used as a loading control.

In order to evaluate a possible functional interaction between CA IX and CAND1 in ribosomal biogenesis too, I performed a ChIP assay on the pre-rRNA 45S gene in SH-SY5Y sh2555.5 stable clone interfered with CAND1 and in ShNS cells, grown under normoxic conditions. ChIP experiments showed that in sh2555.5 cells the recruitment of CA IX on the pre-rRNA 45S gene was strongly decreased (orange bars) compared to shNS cells (yellow bars) (Figure 28). These data suggest that decreased CAND1 expression levels indeed affect CA IX levels and its binding to the chromatin, thus suggesting that the physical interaction between the two proteins does indeed suggest a functional association for the CA IX/CAND1 complex.

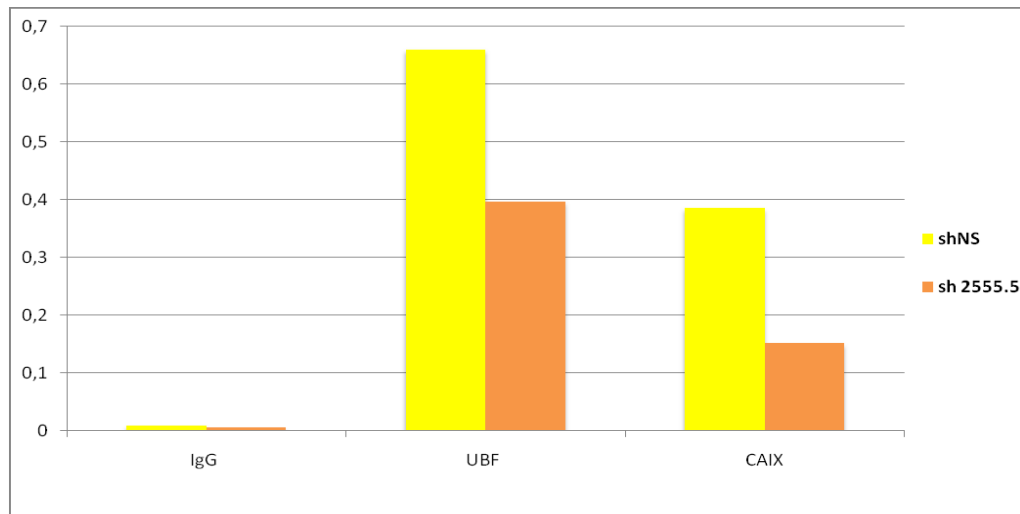


Figure 28. Chromatin-Immunoprecipitation assay rRNA 45S gene in SH-SY5Y stable clone interfered with CAND1. The binding of CA IX on the pre-rRNA 45S gene is strongly decreased (orange bars) compared to shNS cells (yellow bars).

3.6 Possible role of CA IX and CAND1 in survival of hypoxic neuroblastoma cells

Generally, the expression of CA IX is linked to hypoxia, and because it is a condition of cellular stress, we can assume that CA IX can have a protective function in hypoxic cells. In order to assess whether really CA IX participates to the mechanisms of cell survival under hypoxic conditions, I tried to manipulate CA IX levels in SH-SY5Y cells by shRNA-mediated silencing and by overexpression with a vector containing the full-length CA IX sequence. I was not able to obtain cells with down-regulated CA IX (data not shown), while I was able to efficiently overexpress CA IX. I then used CA IX-overexpressing cells to detect cell death by the annexin-V. Fluorescein-conjugated Annexin V(FITC) is indeed capable to bind the phosphatidylserine (PS), a phospholipid normally present in the inner side of the cell membrane. When the PS is exposed outside the membrane, because there is an apoptotic or necrotic event, it can be revealed by the annexin V conjugate. The histogram of figure 29 shows the comparison between control cells and cells overexpressing CA IX, under

normoxic and hypoxic conditions. In normoxia (blue bars), in cells overexpressing CA IX and control cells there was a similar percentage of cells positive to annexin-V (25% and 21% respectively); following hypoxia (red bars), the percentage of cells positive to annexin-V was lower in cells overexpressing CA IX than in control cells (31% and 43%, respectively).

These data suggest that cells overexpressing CA IX are protected from the hypoxic insult, compared to cells expressing endogenous levels of CA IX protein.

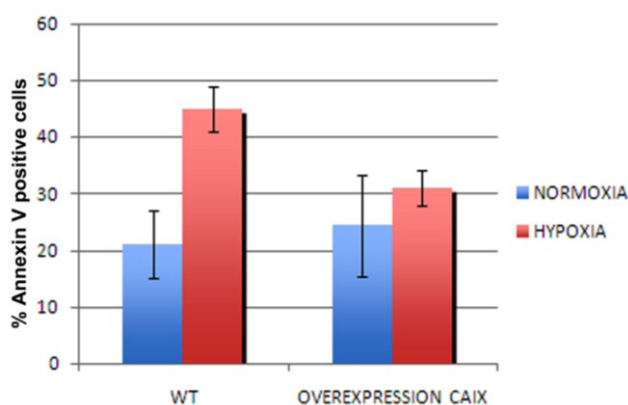


Figure 29. Annexin V assay of SHSY5Y wild type cells and of cells that overexpress CA IX, under normoxic and hypoxic conditions. In hypoxia, the percentage of cells positive for annexin-V is lower in cells that overexpress CA IX than in control cells.

A similar assay was performed in two different clones stably interfered with CAND1, namely sh2555.5 and sh2562.7, where it is known that CA IX is downregulated, and in a population of control, shNS (Figure 30). In normoxia (blue bars), the percentage of cell death in shNS and sh2555.5 clones is comparable, whereas sh2562.8 clone presents a higher percentage of

damaged cells. In hypoxia, the percentage of positive cells was higher in the two clones interfered for CAND1, compared to control cells.

Figure 31 show the results of the western blot analysis performed to validate the downregulation of CAND1 of the two clones interfered. sh2555.5 and sh2562.7 clones showed a decreased level of CAND1 compared to shNS clone.

These data suggest that the overexpression of CA IX protects cells against cell death while the deficiency of CAND1, with a consequent decrease in CA IX levels, leads to an increased sensitivity to cell death.

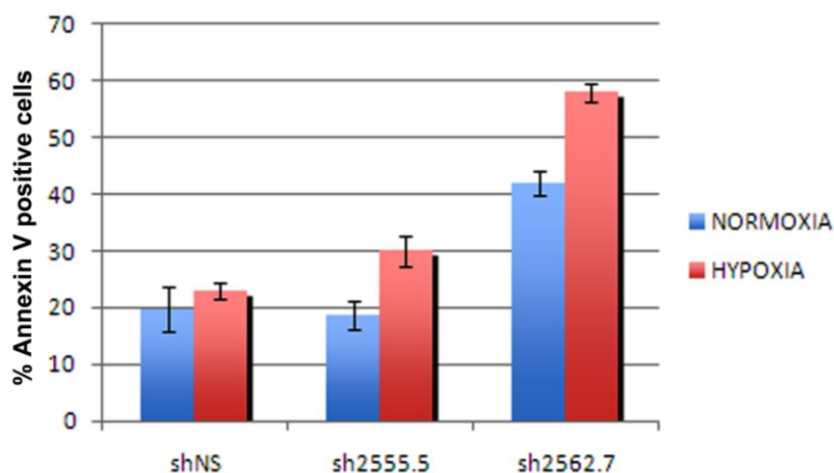


Figure 30. Annexin V assay of clones stably interfered with CAND1. In hypoxia, the percentage of positive cells is greater in the two clones interfered with CAND1 than in control cells.

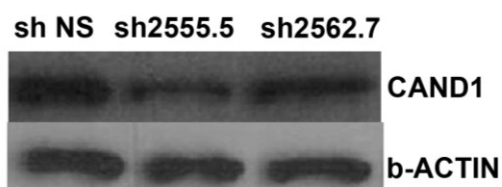


Figure 31. CAND1 downregulation in SH-SY5Y stable clones. CAND1 is downregulated in sh2555.5 and sh2562.7 compared to shNS clone.

3.7 Carbonic anhydrases in *C. elegans*

The redundancy of carbonic anhydrases in mammals prevents to analyze the functions of these enzymes *in vivo*. In fact, CA9-knock out mice show mild behavioural phenotypes¹¹⁸. On the other hand, the *C. elegans* model revealed a precious system for the analysis *in vivo* of hypoxic and anoxic stresses. Thus, in order to evaluate whether the nematode *C. elegans* possesses a human CA9 orthologue gene, I performed an *in silico* analysis, using a free bioinformatic tool, named Phobius (phobius.sbc.su.se), which is currently used for prediction of transmembrane topology and signal peptides from the amino acid sequence of a protein. This analysis revealed that, among the several carbonic anhydrase genes in *C. elegans*, only *cah-5* does indeed possess a putative transmembrane region, from amino acid 285 to position 309, and a corresponding topology, compared to CA IX (Figure 32).

Prediction of sp|Q10462|CAH5_CAEEL

ID sp|Q10462|CAH5_CAEEL
FT SIGNAL 1 20
FT REGION 1 4 N-REGION.
FT REGION 5 16 H-REGION.
FT REGION 17 20 C-REGION.
FT TOPO_DOM 21 284 NON CYTOPLASMIC.
FT TRANSMEM 285 309
FT TOPO_DOM 310 310 CYTOPLASMIC.

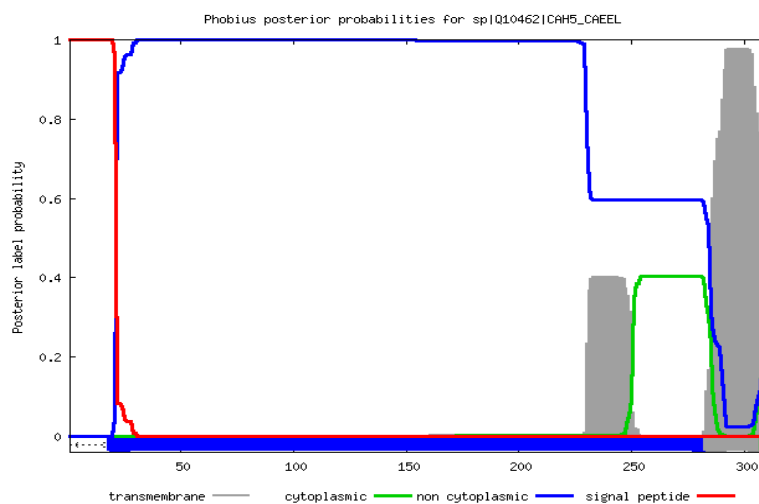


Figure 32. Prediction of transmembrane topology and signal peptides from the amino acid sequence of CAH-5. Bioinformatic analysis reveal that a putative transmembrane helix is in the 285-309 region of the protein. At the bottom, the plot shows, with different colors, the posterior probabilities of cytoplasmic (green) /non cytoplasmic (blue) /TM helix (gray)/signal peptide (red) regions of CAH-5.

On the other hand, it is largely known that *cah-6* is strongly expressed in the nervous system of the nematode.

So, I decided to investigate the role of these two carbonic anhydrases *in vivo*, in response to hypoxic and/or anoxic stimuli. To this aim, I generated worms in which *cah-5* or *cah-6* genes were silenced by *RNA interference by feeding*. In particular, regions of cDNA of carbonic anhydrase genes were cloned between two inverted T7 RNA polymerase promoters. The IPTG induction of the bidirectional transcription generated a dsRNA in the bacterial host, so in the worm fed with this bacteria the specific carbonic anhydrase were down-regulated.

A first group of wild-type worms (P0 generation) were fed bacteria carrying the dsRNA for *cah-5* and exposed to hypoxic (0.5% oxygen) or anoxic (<0,1% oxygen) conditions, in order to evaluate the effects of the treatment in the F1 generation (Figure 33). In normoxic conditions worms interfered by *cah-5* didn't show relevant phenotypes, in comparison to the control worms.

In hypoxic conditions the interfered worms showed a lower embryonic lethality compared to the control worms, in which the lethality was about 15%. In anoxic conditions, no differences were observed between the two groups of worms, in terms of embryonic lethality. These data suggest that *cah-5* gene exacerbates the embryonic lethal phenotype in hypoxic worms, but not in anoxic ones.

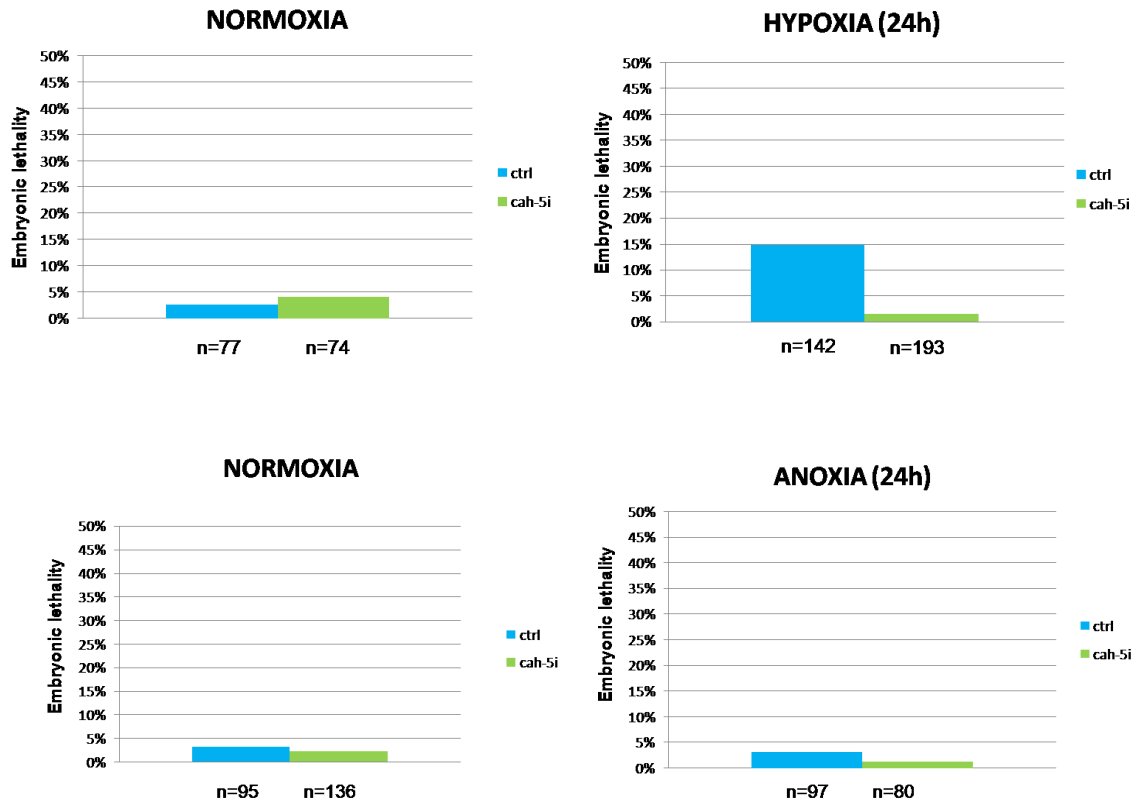


Figure 33. Embryonic lethality phenotype observed in worms interfered for *cah-5* gene. In normoxic conditions worms interfered by *cah-5* didn't show relevant phenotypes, in comparison to the control worms. Under hypoxic condition, worms interfered for *cah-5* gene show a lower embryonic lethality compared to the control worms. In anoxic conditions, no differences were observed between the two groups of worms.

A second group of wild-type worms (P0 generation) were silenced for *cah-6* gene and exposed to anoxic (<0,1% oxygen) conditions, in order to study the phenotypes of the F1 generation.

In these worms, we assayed two phenotypes, namely, embryonic lethality and the capacity of the hermaphrodites to lay eggs (Figure 34).

Under normoxic conditions, both wt and silenced worms showed a low embryonic lethality and were able to lay a large, consistent number of eggs. Conversely, in anoxic conditions the silenced worms showed a higher

embryonic lethality and defects in the egg laying, compared to the control worms.

These data suggest that normally *cah-6* gene protects worms against embryonic lethality and egg-laying defects during anoxia.

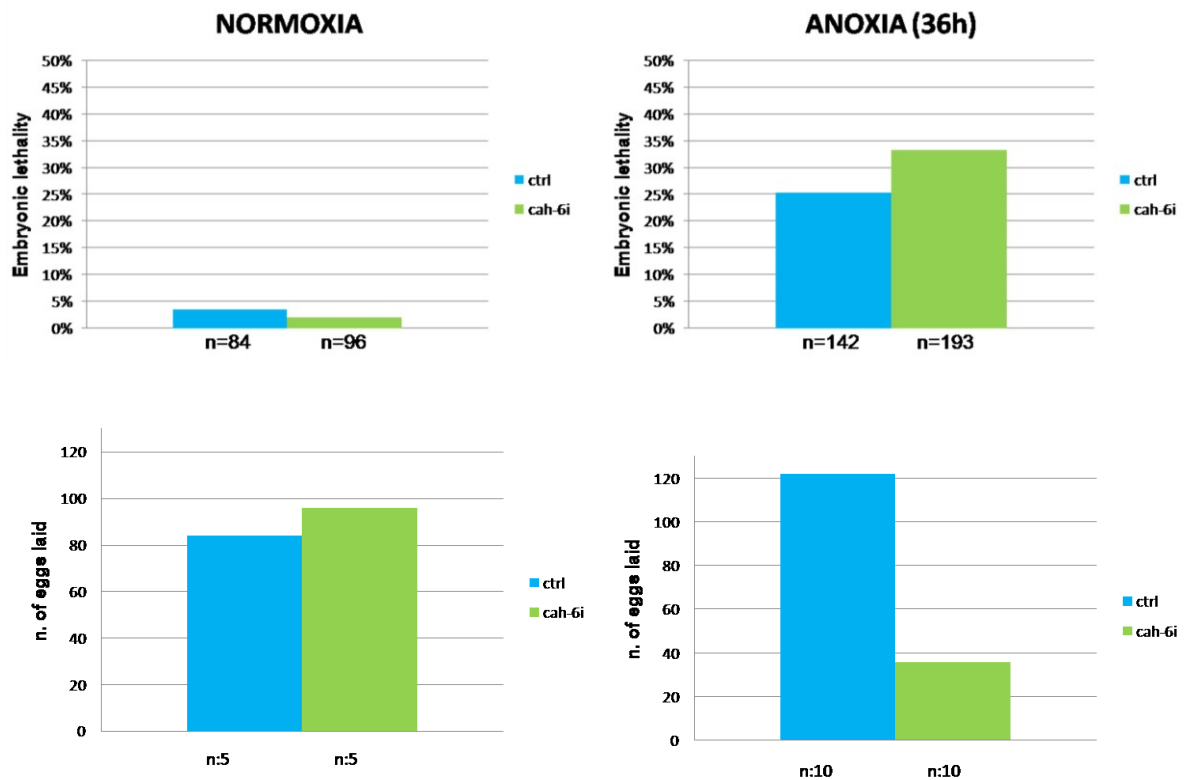


Figure 34. Embryonic lethality phenotype and defects in the egg laying observed in worms interfered for *cah-6* gene. In normoxic conditions, both control and silenced worms showed a low embryonic lethality and were able to lay eggs. In anoxic conditions, the interfered worms showed a higher percentage of embryonic lethality and defects in the egg laying, compared to the control worms.

4. DISCUSSION

Hypoxia is a state of oxygen deficiency, in tissues and cells, sufficient to impair functions of the brain and other organs. A consequence of this deprivation is a decrease of the intracellular pH of neurons and glial cells. The maintenance of an adequate pH is a key factor in the functioning of the Central Nervous System. It is relevant to better understand the pathways involved in the response to hypoxia and the processes that occur in mature neurons, in order to find possible players that can prevent neurodegeneration and trigger cell survival pathways.

CA IX is a transmembrane protein, overexpressed in hypoxic cells, involved in pH and in survival regulation.

Studying the interactome of CA IX, it was found that most of its interactors, especially in hypoxia, belong to the nucleo-cytoplasmic transport machinery.

Immunofluorescence analyses in undifferentiated SH-SY5Y neuroblastoma cell line revealed a surprising nuclear distribution of CA IX protein and this distribution was even more prominent in the differentiated counterpart.

This unexpected subcellular localization was also observed in mouse embryonic stem cells differentiated into neurons. This suggests that CA IX doesn't perform its function only at level of the membrane, but it can participate to so far unidentified mechanisms during neuronal differentiation and neuronal responses to hypoxia.

A hypothetical nuclear function for CA IX was occasionally postulated on the basis of its ability to bind DNA in DNA-cellulose chromatography ¹⁷. Since then, no additional reports focused on nuclear CA IX localization and/or functions. Bioinformatic analysis highlighted the presence of a stretch of basic amino acids able to bind DNA. CHIP experiments described in this PhD thesis, propose a novel nuclear function of CA IX, more specifically in the nucleoli, and in the ribosomal RNA biogenesis. Indeed, I found CA IX bound to the promoter of the pre-rRNA 45S gene, although it is still unclear whether this is a direct interaction with DNA, or whether adaptor proteins are involved. Still unclear is the

functional significance of CA IX association to this promoter, although it appears inversely correlated to UBF occupancy, and decreased during hypoxia. Further experiments will be required to evaluate rRNA 45S expression during hypoxia and neuronal differentiation for proper association to ChIP data.

It is known that the components of the nucleus-cytoplasmic transport play an important role in response to hypoxia to assist in the proper location of all the key factors that regulate cellular changes in response to hypoxic condition ¹¹⁹⁻¹²¹. Hypoxia also leads to changes in ribosome biogenesis, translation efficiency and protein degradation ¹²². So hypoxia modulates many of the pathways in which interactors of CA IX are involved, and this provides additional support to the experimental evidence described.

Within the IC region of CA IX (aa 418-459) were identified hypothetical sequences NLS and NES, through the use of bioinformatics software.

I verified that these sequences were actually able to drive the localization of GFP reporter protein in SH-SY5Y cells. Namely, the presence of the NLS sequence alone favors an accumulation of CA IX within the nucleus. The reporter protein containing NES+NLS the sequence is expressed with lower efficiency, but the combined signals clearly result in the nuclear exclusion and in the cytosolic accumulation of the GFP. This could be due to a dominant effect of the NES sequence on the NLS. However, these data demonstrate that both sequences can actually act as a localization signals, so that their presence in the CA IX sequence may justify its nuclear trafficking.

It is indeed not unusual, for a membrane protein, to be able to traffic to the nucleus, in fact there are other similar cases described in the literature: c-Erb-B2, EGFR, FGFR and CD44 ¹²³⁻¹²⁵. The nuclear localization of these proteins requires prior transit in the membrane and their recycling through the endocytic pathway ¹²⁴, before nuclear accumulation. Once in the nucleus, these proteins, including CA IX, now devoid of membrane vesicles, may expose the putative NES for further recycle to extranuclear compartments.

CAND1 is a nuclear protein previously associated both to the recruitment of general factors to initiate transcription by RNA polymerase II, and to the assembly of SCF ubiquitin E3 ligase complexes, involved in the degradation of specific proteins by the proteasome 26S. Since interaction of CA IX with CAND1 is more abundant during hypoxia, I postulated a functional significance for this interaction in the increased stability of the carbonic anhydrase during hypoxic stress.

Biochemical data presented in this thesis indeed confirmed the interaction of CA IX and CAND1 in native complexes. Functional interaction between these two proteins was also validated in SH-SY5Y cell clones expressing stable decreased levels of CAND1 protein through RNA interference. In fact, when CAND1 was downregulated, CA IX expression decreased, both in normoxia and in hypoxia. CHIP experiments indeed paralleled this correlation, since CA IX showed a decreased chromatin association in the presence of down-regulated CAND1. These data strongly support the hypothesis that CAND1 levels actually affect CA IX stability.

Cell death assays finally revealed that CA IX is involved in cell survival and plays a protective role against hypoxic stress; this function is abolished in cells expressing low levels of CAND1, in which CA IX is down-expressed. Unfortunately, I was not able to raise CA IX down-regulated clones. This can be probably explained, because of the suggested role for CA IX in cell survival, which prevents from selection of CA IX down-regulated cells.

Finally, a preliminary characterization of two carbonic anhydrases of the nematode *Caenorhabditis elegans* was performed. A bioinformatic screening of the nematode genome for membrane-associated carbonic anhydrases revealed CAH-5 as a possible CA IX orthologue. Also CAH-6 was selected, as an additional carbonic anhydrase family member, not associated to the membrane. Using RNAi approach, *cah-5* and *cah-6* transcripts were down-regulated in the parental generation in order to study the phenotypes in the F1 generation. The most relevant defect were embryonic lethality and reduced egg laying.

Interestingly, worms silenced for *cah-5* show different phenotypes during hypoxia and anoxia. Indeed, under normoxia and anoxia condition interfered worms didn't show relevant phenotypes, whereas under hypoxia interfered worms show a lower level of embryonic lethality. In all three condition, these worms didn't show defects in egg laying (data not show).

These data suggest that *cah-5* may have a role in the correct development of the embryos, in particular in the early stages and that the presence of *cah-5* gene exacerbates the embryonic lethal phenotype in hypoxic worms, but not in anoxic ones. It is interesting to note that worsening of a phenotype as a consequence of hypoxia was also shown by *hif-1* mutant null worms in which, a lower level of axon-pathfinding defects were observed, compared to wild-type worms. So, it can be postulated that *cah-5* acts as a target and an effector of HIF1, selectively during hypoxia, in *C. elegans*. In fact, in the worm hypoxia and anoxia are independent environmental conditions, and they are accordingly controlled by independent pathways.

Worms silenced for *cah-6* were less able to lay eggs, under anoxic condition. Furthermore in this condition, these worms present a high embryonic lethality. These data suggest that *cah-6* may act in the late intra-uterine stages of development protecting worms against embryonic lethality and egg-laying defects and that it may control the activity of neurons involved in the egg laying, such as HSN or VCs motoneurons or acts on egg laying muscles contraction. In the present thesis work, experiments were presented, highlighting additional, molecular and functional features of carbonic anhydrase IX.

Besides its involvement in cellular functions at the cell membrane, my data demonstrated that CA IX may work as a nuclear protein. It indeed interacts with the whole set of proteins, responsible for trafficking towards, and outwards the nuclear compartment. Its nuclear localization is particularly relevant in the neuronal cell models analyzed, where it may support survival under differentiating conditions and during hypoxic stress. The latter function is highly promising towards the identification of molecules with the ability to activate CA IX functions in pathological conditions dealing with hypoxia, such as stroke.

Thus, molecular characterization of the complexes of CA IX with selected interactors, such as CAND1, which is indeed responsible for its stabilization at the protein level, may be helpful to design small molecule activators of carbonic anhydrase IX with innovative therapeutic potential.

5. MATERIALS AND METHODS

5.1 Cell lines, *Caenorhabditis elegans* maintenance and experimental treatments

The HEK-293, SH-SY5Y, BJ5T α and GEO cell lines were purchased from ATCC. Cells were cultured in DMEM containing 10% fetal bovine serum (Euroclone) and penicillin/streptomycin, 2mM glutamine at 37°C, in 5% CO₂ humidified atmosphere.

Transient transfection of HEK-293 cells with the empty vector, pRcCMV, or the strep-tagged CA IX vector have been performed at a confluence of 70% using the calcium phosphate method. At 24 hours after transfection a group of cells was maintained under normoxic conditions while another one was subjected to hypoxic treatment, for sixteen hours, in an incubator with N₂ atmosphere containing 2% O₂ and 5% CO₂.

A day before retinoic acid (RA; Sigma) treatment, SH-SY5Y cells were cultured in DMEM containing 2% fetal bovine serum (Euroclone) and penicillin/streptomycin, 2mM glutamine at 37°C, in 5% CO₂ humidified atmosphere. After this, the RA were added to media at a final concentration of 10 μ M for cells to be differentiated; control cells were treated with DMSO (0.1%).

For analysis of putative NES and NLS CA IX sequences SH-SY5Y cells were transfected with the same method previous described. After 24 hours cells transfected with the constructs containing the NLS or NES+NLS sequences were grown in hypoxia for six hours or maintained under normoxic conditions. The hypoxic treatment were performed in a hypoxia chamber (Hypoxia Incubator Chamber, STEMCELL Technologies), blowing the gas (95% N₂ and 5% CO₂, 1.6 psi) for 4 minutes. The same treatment was repeated after 30 minutes in order to expel all the O₂ in the chamber.

For annexin-V assay SH-SY5Y culture at a confluence of 70% was transfected using Lipofectamine (Lipofectamine 2000 Transfection Reagent, Invitrogen) with

the empty vector, pRcCMV or with the same vector containing the full-length CA IX gene sequence.

SH-SY5Y were transfected with pSM2 vectors containing shRNAs targeting CAND1 mRNAs to interfere their expression. Stable clones were established by treating cells for two weeks with 2 µg/ml of puromycin and amplified using 0.2 µg/ml of puromycin to maintain stable expression of constructs.

E14Tg2a (BayGenomics) mouse ES cells were maintained on feeder-free, gelatine coated plates in GMEM (Sigma) containing 2mM glutamine (Invitrogen) 100U/ml penicillin/streptomycin (Invitrogen), 1mM sodium pyruvate (Invitrogen) 1x non essential amino acids (Invitrogen) 0.1 mM β-mercaptoethanol (Sigma) 10% FBS (Hyclone) and 10³ U/mL leukemia inhibitory factor (LIF) (Chemicon).

For neural differentiation cells were trypsinized into a single cells suspension and seeded at the density of 3x10³ cells for cm². Cells were cultured in Knockout Dulbecco's minimal essential medium containing 10% Knockout Serum Replacement (all from Invitrogen) 0.1 β-mercaptoethanol, 2 mM glutamine, 100 U/mL penicillin-streptomycin.

Finally, nematodes were cultured at 20°C on Normal Growth Media (NGM) agar plates seeded with OP50 or Ht115 *E. coli* bacteria.

For hypoxic treatment worms were maintained for 24 hr in the hypoxic chamber with 95.5% N₂ and 0.5% O₂, while for anoxic treatment worms were maintained for 24 or 36 hr with 95% N₂ and 5% CO₂.

5.2 DNA constructs

The expression construct encoding the full-length CA IX protein was obtained by RT-PCR amplification of mRNA isolated from non small cell lung cancer explanted tumors with ImProm-II Reverse transcriptase (Promega) and Pfu DNA polymerase. The primers for cDNA amplification were synthesized at CEINGE oligonucleotide facility and were the following: ca9for, 5'-cacaagcttagccgccatggctcccctgtgccccagc-3'; ca9rev, 5'-cactctagattatcctcctccttttgaactgcgggtggctccaggctccatctcggctacctc-3'. The last oligonucleotide contained additional bases encoding for the Strep-tag II

sequence WSHPQFEK, through which recombinant protein was tagged. The PCR product was cloned in the pRcCMV vector (Invitrogen). cDNA was fully sequenced for verification.

Constructs containing NLS and NES+NLS sequences, canonical and CA IX putative, were generated in frame-fusing them at the C-terminus of EGFP in the vector of expression pEGFP_C1.

The construct pEGFP_NLS-SV40 (TAg) was generated through annealing of the following synthetic oligonucleotides: NLS_SV40 (TAg) _US: 5'-GATCTCCAAAAAGAAGAGAAAGGTAG-3'; NLS_SV40 (TAg) _LS: 5'-TCGACTACCTTTCTCTTCTTTTTTGGGA-3';

The construct pEGFP_canonicalNES+NLS was produced using a synthetic forward oligonucleotide as template and a reverse oligonucleotide as primer to copy the template: NES_NLS_can_US: 5'-ATAAGATCTCCAAAAAGAAGAGAAAGGTAGGATCCGGCGGCGGCTTAGCCTTGAAATTAGCAGGTCTTGATATC-3'; NES_NLS_can_Rev: 5'-ACTGTAGTCGACGATATCAAGACCTGCTAATTTTC-3'.

The constructs pEGFP_CA IX putative NLS and pEGFP_CA IX putativeNES+NLS, encompassing sequence from 434 to 459 and from 412 to 459 of the full length protein, respectively, were generated by PCR from cDNA of full length CA IX using the following oligonucleotides: CA9_Cterm_For: 5'-ATAAGATCTGGTGACATCCTAGCCCTGGT-3'; CA9_Cterm_Rev: 5'-ACTGTAGTCGACGGCTCCAGTCTCGGCTACCT-3'; CA9_IC_For: 5'-ATAAGATCTCAGATGAGAAGGCAGCACAGA-3'; CA9_Cterm_Rev: 5'-ACTGTAGTCGACGGCTCCAGTCTCGGCTACCT-3'.

Forward oligonucleotides contained the restriction site for BglII, whereas reverse oligonucleotides possessed the restriction site for Sall. They have been synthesized at CEINGE oligonucleotide facility and fully sequenced for verification.

The pSM2 vector containing the shRNAs 2555 (5'-TGCTGTTGACAGTGAGCGCGCAATGTAGATGATGATGAATTAGTGAAGCCACAGATGTAATTCATCATCATCTACATTGCATGCCTACTGCCTCGGA-3')

targeting CAND1 mRNAs, together with the non silencing shNS construct, were selected from a library of shRNAs generated by Dr. Greg Hannon at Cold Spring Harbor Laboratory (CSHL) and provided us by the Open Biosystems. These shRNAs were designed to be expressed as human microRNA-30 (miR30) primary transcripts to increase Drosha and Dicer processing of the expressed hairpins and consequently knockdown efficiency. Briefly the hairpin stem consists of 22-nt of dsRNA, complementary to mRNA target, the loop is formed by 19-nt from human miR30; the 125-nt of flanking sequence on either side of the hairpin are also from miR30.

The 22-nt dsRNA portion of the shRNAs targeting CAND1 mRNAs is complementary to sequences present in the coding region.

For the RNAi experiments, worms were fed with HT115 *E. coli* cells expressing dsRNA for *cah-5* and *cah-6* or with the pL4440 empty vector (population of control).

The fragment of *cah-5* and *cah-6* were generated by PCR from genomic DNA extracted from a mixed-stage population of N2 (wild type) strain. The primers for *cah-5* amplification were: CE_cah-5_RNAi_For TTCACGTGGCTGCGAGAATGAAA; CE_cah-5_RNAi_Rev AAACGCGACGCACAAAAGGTCA. The primers for *cah-6* amplification were: CE_cah-6_RNAi_For CCCACCAACCATGGCATTCC; CE_cah-6_RNAi_Rev CCCAGTCTCATTGACTAACCTG.

The *E. coli* cells were transformed with the pL4440 vector containing the sequences amplified. NGM plates containing 50mg/ml ampicillin (mp) and 1mM IPTG seeded with transformed bacterial cultures (grown overnight in LB). After the induction of the dsRNA expression performed overnight at RT, synchronized worms were transferred to the plates and were kept at 20°C.

5.3 Cell lysates preparation, interactome characterization and mass spectrometry protein identification

Cells were lysated in a buffer containing 50 mM Tris-HCl, 150 mM NaCl, 0,5% Triton X-100, 10% glycerol, pH 7.5, 50 mM NaF, 1 mM Na₃VO₄, 1 mM DTT, 0,4 mM EDTA, pH 8.0, and a mixture of protease inhibitors (Sigma Aldrich) ¹²⁶. Lysates were clarified by centrifugation at 12,000 g for 20 min at 4 °C and quantified using BioRad Protein Assay, based on the Bradford method, following the manufacturer's instructions.

Each lysate (2 mg) was challenged with 250 µL of Strep-Tactin resin (IBA), and incubated for 12 h, at 4 °C. After washing, proteins were eluted with 100 mM Tris-HCl, 150 mM NaCl, 1 mM EDTA, 0.1% Triton X-100, 2 mM D-biotin, pH 8. Interactors eluted with CA IX were analyzed by 12% SDS-PAGE (14 cm × 16 cm × 0.75 mm) in an SE600 vertical electrophoresis system (Hoefer), at 18 °C, using a constant current setting of 25 mA and a maximum of 150 V.

Detection of proteins was performed by silver nitrate staining. Gel images were scanned by the Image Scanner III (GE Healthcare) apparatus and analyzed by the Image Master 2D Platinum 6.0 software (GE Healthcare), according to the manufacturer's instructions.

Each gel lanes from SDS-PAGE was cut and subdivided into 21 slices, which were then processed for downstream protein identification by mass spectrometry. Peptide digests of interactors were analyzed by nLC-ESI-LIT-MS/MS. MS analysis was performed by Dr. G. Renzone and A. Scaloni, ISPAAM, CNR, Naples.

5.4 Bioinformatic analysis

Proteins identified by nLC-ESI-LIT-MS/MS were analyzed using the String v. 9.0 database (<http://string-db.org/>) to discover functional interaction between them. A classification of the identified proteins under parameters of gene ontology was performed through the web-accessible DAVID (v 6.7) annotation system (<http://david.abcc.ncifcrf.gov/home.jsp>).

A bioinformatic analysis of CA IX C-terminal region to find putative NES and NLS sequences was performed using the predictive software NetNES 1.1 Server (<http://www.cbs.dtu.dk/services/NetNES/>) and NLStradamus (<http://www.moseslab.csb.utoronto.ca/NLStradamus/>), respectively.

Prediction of transmembrane topology and signal peptides of the carbonic anhydrases of *Caenorhabditis elegans* was performed using the predictive software Phobius (phobius.sbc.su.se)

5.5 Antibodies, interaction assays and western blot analysis

Antibodies used in biochemical experiments were the following: CA IX VII/20 and M75, mouse monoclonals; CA IX, rabbit polyclonal (H-120, Santa Cruz Biotechnology); XPO1 (CRM1 C-20, Santa Cruz Biotechnology), goat polyclonal; CAND1 (TIP120A 48, Santa Cruz Biotechnology), mouse monoclonal, β 3-tubulin (TU-20, Santa Cruz Biotechnology), mouse monoclonal and β -actin (AC-15, Santa Cruz Biotechnology), mouse monoclonal.

Affinity purification experiments were performed on 1mg of protein extracts on Strep-Tactin resin for 2 hours, at 4°C. Elution was preceded by 5 washes with lysis buffer. Eluates were analyzed by 10% SDS-PAGE.

Co-immunoprecipitation experiments for analysis of CA IX-CAND1 native complexes were performed using an anti- CA IX antibody; immunocomplexes were captured by protein A/G plus agarose (Santa Cruz Biotechnology) and, once eluted, subjected to western blot analysis.

5.6 Fluorescence and immunofluorescence analyses

Immunofluorescence experiments were performed on HEK-293, SH-SY5Y, GEO and BJ5T α cells.

Cells used for analysis were platen on glass slides and, after being subjected to various treatments described in previous sections, fixed with 3% (w/v) paraformaldheyde, 1% (w/v) sucrose in PBS for 20 min. after washes with PBS

cells were permeabilized with 0.3% (w/v) Triton X-100 in PBS for 3 min, at 4 °C. Cells were then incubated with appropriate dilution of primary antibody CA IX VII /20, mouse monoclonal and/or . To visualize by fluorescence target protein, cells were incubated for 1h at 25°C with the secondary antibody Alexa-488-conjugated rabbit antimouse (Jackson Laboratories).

Fluorescence analysis at confocal microscope (Zeiss LM510) was performed on SH-SY5Y cells transfected with the constructs containing GFP fused at the C-terminus with CA IX NES and NLS sequences. Cells were fixed with 3% (w/v) paraformaldehyde, 1% (w/v) sucrose in PBS for 20 minutes at room temperature (RT). Nuclei were stained with DRAQ5 (anthracinone dye for far-red nuclear staining) and the signal was detected exciting cells with a wavelength of 647 nm).

For immunofluorescence of ESCs, the cells were fixed in 4% paraformaldehyde and permeabilized with 0.2% TX-100 in FBS (Invitrogen)/1% BSA in 1X PBS for 15 minutes at RT. The cells were incubated with primary antibodies at the following working dilutions: anti β 3-tubulin (1:400 Sigma), anti-Oct3/4 (1:200; Santa Cruz), anti-Sox1 (1:100: Santa Cruz). Following primary antibodies incubation, the cells were incubated with appropriate secondary antibodies detecting mouse, rabbit and goat rat IgG conjugated with Alexa Flour 594 or 488 (molecular Probes). Images were captured with an inverted microscope (DMI4000, Leica Microsystems).

5.7 Chromatin Immunoprecipitation

Cells were treated with 1% formaldehyde for 10 minutes at RT. Then, formaldehyde was inactivated adding 125mM Glycine. Chromatin was sonicated to an average DNA-fragment of 200-1,000 bp. Soluble chromatin extracts were immunoprecipitated using CA IX and UBF antibodies and mouse IgG as control. Supernatant obtained without antibody was used as input control. The amount of precipitated DNA was detected by real-time PCR relative to total input chromatin, and expressed as percent of total chromatin according

to the following formula: $2^{\Delta Ct} \times 10$, where Ct represents the cycle threshold and $\Delta Ct = Ct (\text{input}) - Ct (\text{immunoprecipitation})$.

All experiments have been done as independent triplicates and to measure statistical significance was used the Student's t-test.

Oligo sequences used to amplifying loci were: 45S pre-rRNA_RealTime_FOR CTCCGTTATGGTAGCGCTGC and 45S pre-rRNA_RealTime_REV GCGGAACCCTCGCTTCTC for region 1; 45S pre-rRNA_RealTime_FOR CTTCGGTCCCTCGTGTGTC and rDNA_45S_prom_ChIP_REV2 GCCCGTGTCTCCAGAGC for region 2.

All primers were used to a final concentration of 4 μM in a 20 μL Real Time reaction containing 10 μL of syber Green 2X (Applied Biosystem) and 2 μL DNA.

5.8 Analysis of cell death

For the analysis of cell death, SH-SY5Y cells were seeded in MW24 plates and transfected with Lipofectamie 2000. Upon 48 hr from the transfection, a group of cells was maintained under normoxic conditions while another one was subjected to hypoxic treatment.

Phosphatidylserine externalization was detected by annexin V.

At least 100,000 cells were collected with PBS-EDTA, and incubated with annexin V-fluorescein isothiocyanate (FITC) (Pharmingen/Becton Dickinson, San Diego, CA) conjugated in 100 μL binding buffer containing 10 mM HEPES (*N*-2-hydroxyethylpiperazine-*N'*-2-ethanesulfonic acid)/NaOH pH 7.5, 140 mM NaCl, 2.5 mM CaCl_2 for 15 minutes at room temperature in the dark. Subsequently, 400 μL of the same buffer was added to each sample and the cells were analyzed in the Becton Dickinson FACScan flow cytometer..

5.9 Measuring Egg Laying and Embryonic Lethality in *C.elegans*

After synchronization of wild type worms by NaOH/chlorine bleaching, the eggs were transferred to plates seeded with HT115 bacteria expressing the pL4440 empty vector or the pL4440 containing fragment of *cah-5* or *cah-6* gene. At the stage of gravid hermaphrodites, individual animals were moved to small NGM plates. The rate of egg laying and the total number of animals alive were measured at different time point with a last observation after 30-40 hr, both in normoxia and in hypoxia/anoxia.

For embryonic lethality evaluation, the total number of eggs unhatched and the total number of nematodes alive were numbered at different time point, with a last observation after 30-40 hr, both in normoxia and in hypoxia/anoxia.

6. ACKNOWLEDGEMENTS

First of all, I want to thank my husband Basilio and my son Emanuele, for all the support and love that they have given me in these years.

A thanks goes to my tutor Prof. Nicola Zambrano. Since 2003, when I took my first lesson of molecular biology, he has my consideration and respect, thanks to his passion for research, scientific competence and patience!

A big thanks goes to my colleagues and lab. friends: Francesca, Pasquale, Stefano, Mariangela Succoio, Mariangela Sabatella, Emanuele, Bianca and Luca. Thanks for your consideration, support and friendship!

I want to thanks Prof. Garbi, Prof. Romano, Dr Silvia Parsi, Dr. Minopoli, Simona and Margherita for scientific support.

Finally, thank to all my family!

7. REFERENCES

1. Thiry, A.; Dogne, J. M.; Masereel, B.; Supuran, C. T., Targeting tumor-associated carbonic anhydrase IX in cancer therapy. *Trends Pharmacol Sci* **2006**, *27*, (11), 566-73.
2. Supuran, C. T.; Scozzafava, A.; Casini, A., Carbonic anhydrase inhibitors. *Med Res Rev* **2003**, *23*, (2), 146-89.
3. Supuran, C. T., Scozzafava, A. & Conway, J., Carbonic Anhydrase - Its inhibitors and Activators *CRC, Boca Raton* **2004**, 1-363.
4. Stams, T. C., D. W., The Carbonic Anhydrases - New Horizons **Birkhauser, Basel**, **2000**, 159-174.
5. Smith, K. S.; Ferry, J. G., Prokaryotic carbonic anhydrases. *FEMS Microbiol Rev* **2000**, *24*, (4), 335-66.
6. Scozzafava, A., Mastrolorenzo, A. & Supuran, C. T., Carbonic anhydrase inhibitors and activators and their use in therapy. *Expert Opin. Ther. Pat.* **2006**, *16*, 1627-1664
7. Pastorekova, S.; Parkkila, S.; Pastorek, J.; Supuran, C. T., Carbonic anhydrases: current state of the art, therapeutic applications and future prospects. *J Enzyme Inhib Med Chem* **2004**, *19*, (3), 199-229.
8. Sly, W. S.; Hu, P. Y., Human carbonic anhydrases and carbonic anhydrase deficiencies. *Annu Rev Biochem* **1995**, *64*, 375-401.
9. Vullo, D.; Voipio, J.; Innocenti, A.; Rivera, C.; Ranki, H.; Scozzafava, A.; Kaila, K.; Supuran, C. T., Carbonic anhydrase inhibitors. Inhibition of the human cytosolic isozyme VII with aromatic and heterocyclic sulfonamides. *Bioorg Med Chem Lett* **2005**, *15*, (4), 971-6.
10. Supuran, C. T.; et al., Carbonic anhydrase inhibitors. Part 29. Interaction of isozymes I, II and IV with benzamide-like derivatives. *Eur. J. Med. Chem* **1998**, *33*, 739-752.
11. Nishimori, I.; Vullo, D.; Innocenti, A.; Scozzafava, A.; Mastrolorenzo, A.; Supuran, C. T., Carbonic anhydrase inhibitors. The mitochondrial isozyme VB as a new target for sulfonamide and sulfamate inhibitors. *J Med Chem* **2005**, *48*, (24), 7860-6.
12. Kohler, K. e. a., Saccharin inhibits carbonic anhydrases: possible explanation for its unpleasant metallic aftertaste. *Angew Chem Int Ed Engl* **2007**, *46*, (40), 7697-9.
13. Sethi, K. K.; Sahoo, S. K.; Pichikala, J. N.; Suresh, P., Carbonic anhydrase I and II inhibition with natural products: caffeine and piperine. *J Enzyme Inhib Med Chem* **2012**, *27*, (1), 97-100.
14. Wykoff, C. C.; Beasley, N. J.; Watson, P. H.; Turner, K. J.; Pastorek, J.; Sibtain, A.; Wilson, G. D.; Turley, H.; Talks, K. L.; Maxwell, P. H.; Pugh, C. W.; Ratcliffe, P. J.; Harris, A. L., Hypoxia-inducible expression of tumor-associated carbonic anhydrases. *Cancer Res* **2000**, *60*, (24), 7075-83.
15. Opavsky, R.; Pastorekova, S.; Zelnik, V.; Gibadulinova, A.; Stanbridge, E. J.; Zavada, J.; Kettmann, R.; Pastorek, J., Human MN/CA9 gene, a novel member of the carbonic anhydrase family: structure and exon to protein domain relationships. *Genomics* **1996**, *33*, (3), 480-7.
16. Nakagawa, Y.; Uemura, H.; Hirao, Y.; Yoshida, K.; Saga, S.; Yoshikawa, K., Radiation hybrid mapping of the human MN/CA9 locus to chromosome band 9p12-p13. *Genomics* **1998**, *53*, (1), 118-9.
17. Pastorek, J.; Pastorekova, S.; Callebaut, I.; Mornon, J. P.; Zelnik, V.; Opavsky, R.; Zat'ovicova, M.; Liao, S.; Portetelle, D.; Stanbridge, E. J.; et al., Cloning and characterization of MN, a human tumor-associated protein with a domain homologous to carbonic anhydrase and a putative helix-loop-helix DNA binding segment. *Oncogene* **1994**, *9*, (10), 2877-88.
18. Barathova, M.; Takacova, M.; Holotnakova, T.; Gibadulinova, A.; Ohradanova, A.; Zatovicova, M.; Hulikova, A.; Kopacek, J.; Parkkila, S.; Supuran, C. T.; Pastorekova, S.; Pastorek, J., Alternative splicing variant of the hypoxia marker carbonic anhydrase IX expressed independently of hypoxia and tumour phenotype. *Br J Cancer* **2008**, *98*, (1), 129-36.

19. Kaluz, S.; Kaluzova, M.; Opavsky, R.; Pastorekova, S.; Gibadulinova, A.; Dequiedt, F.; Kettmann, R.; Pastorek, J., Transcriptional regulation of the MN/CA 9 gene coding for the tumor-associated carbonic anhydrase IX. Identification and characterization of a proximal silencer element. *J Biol Chem* **1999**, 274, (46), 32588-95.
20. Kaluzova, M.; Pastorekova, S.; Svastova, E.; Pastorek, J.; Stanbridge, E. J.; Kaluz, S., Characterization of the MN/CA 9 promoter proximal region: a role for specificity protein (SP) and activator protein 1 (AP1) factors. *Biochem J* **2001**, 359, (Pt 3), 669-77.
21. Kaluz, S.; Kaluzova, M.; Stanbridge, E. J., Expression of the hypoxia marker carbonic anhydrase IX is critically dependent on SP1 activity. Identification of a novel type of hypoxia-responsive enhancer. *Cancer Res* **2003**, 63, (5), 917-22.
22. Grabmaier, K.; MC, A. d. W.; Verhaegh, G. W.; Schalken, J. A.; Oosterwijk, E., Strict regulation of CAIX(G250/MN) by HIF-1 α in clear cell renal cell carcinoma. *Oncogene* **2004**, 23, (33), 5624-31.
23. Black, A. R., Sp1 and Kruppel-like factor family of transcription factors in cell growth and cancer. *J. Cell. Physiol.* **2000**, 188, (2), 143-160.
24. Kopacek, J.; Barathova, M.; Dequiedt, F.; Sepelakova, J.; Kettmann, R.; Pastorek, J.; Pastorekova, S., MAPK pathway contributes to density- and hypoxia-induced expression of the tumor-associated carbonic anhydrase IX. *Biochim Biophys Acta* **2005**, 1729, (1), 41-9.
25. Alterio, V.; Hilvo, M.; Di Fiore, A.; Supuran, C. T.; Pan, P.; Parkkila, S.; Scaloni, A.; Pastorek, J.; Pastorekova, S.; Pedone, C.; Scozzafava, A.; Monti, S. M.; De Simone, G., Crystal structure of the catalytic domain of the tumor-associated human carbonic anhydrase IX. *Proc Natl Acad Sci U S A* **2009**, 106, (38), 16233-8.
26. Hilvo, M.; Baranauskiene, L.; Salzano, A. M.; Scaloni, A.; Matulis, D.; Innocenti, A.; Scozzafava, A.; Monti, S. M.; Di Fiore, A.; De Simone, G.; Lindfors, M.; Janis, J.; Valjakka, J.; Pastorekova, S.; Pastorek, J.; Kulomaa, M. S.; Nordlund, H. R.; Supuran, C. T.; Parkkila, S., Biochemical characterization of CA IX, one of the most active carbonic anhydrase isozymes. *J Biol Chem* **2008**, 283, (41), 27799-809.
27. Pastorekova, S.; Zatovicova, M.; Pastorek, J., Cancer-associated carbonic anhydrases and their inhibition. *Curr Pharm Des* **2008**, 14, (7), 685-98.
28. Zavadova, Z.; Zavadova, J., Carbonic anhydrase IX (CA IX) mediates tumor cell interactions with microenvironment. *Oncol Rep* **2005**, 13, (5), 977-82.
29. Zavadova, J.; Zavadova, Z.; Pastorek, J.; Biesova, Z.; Jezek, J.; Velek, J., Human tumour-associated cell adhesion protein MN/CA IX: identification of M75 epitope and of the region mediating cell adhesion. *Br J Cancer* **2000**, 82, (11), 1808-13.
30. Svastova, E.; Zilka, N.; Zat'ovicova, M.; Gibadulinova, A.; Ciampor, F.; Pastorek, J.; Pastorekova, S., Carbonic anhydrase IX reduces E-cadherin-mediated adhesion of MDCK cells via interaction with beta-catenin. *Exp Cell Res* **2003**, 290, (2), 332-45.
31. Hulikova, A.; Zatovicova, M.; Svastova, E.; Ditte, P.; Brasseur, R.; Kettmann, R.; Supuran, C. T.; Kopacek, J.; Pastorek, J.; Pastorekova, S., Intact intracellular tail is critical for proper functioning of the tumor-associated, hypoxia-regulated carbonic anhydrase IX. *FEBS Lett* **2009**, 583, (22), 3563-8.
32. Dorai, T.; Sawczuk, I. S.; Pastorek, J.; Wiernik, P. H.; Dutcher, J. P., The role of carbonic anhydrase IX overexpression in kidney cancer. *Eur J Cancer* **2005**, 41, (18), 2935-47.
33. Ditte, P.; Dequiedt, F.; Svastova, E.; Hulikova, A.; Ohradanova-Repic, A.; Zatovicova, M.; Csaderova, L.; Kopacek, J.; Supuran, C. T.; Pastorekova, S.; Pastorek, J., Phosphorylation of carbonic anhydrase IX controls its ability to mediate extracellular acidification in hypoxic tumors. *Cancer Res* **2011**, 71, (24), 7558-67.
34. Buanne, P.; Renzone, G.; Monteleone, F.; Vitale, M.; Monti, S. M.; Sandomenico, A.; Garbi, C.; Montanaro, D.; Accardo, M.; Troncone, G.; Zatovicova, M.; Csaderova, L.; Supuran, C. T.; Pastorekova, S.; Scaloni, A.; De Simone, G.; Zambrano, N., Characterization of carbonic anhydrase IX interactome reveals proteins assisting its nuclear localization in hypoxic cells. *J Proteome Res* **2013**, 12, (1), 282-92.
35. Huang, L. E.; Bunn, H. F., Hypoxia-inducible factor and its biomedical relevance. *J Biol Chem* **2003**, 278, (22), 19575-8.

36. Maxwell, P. H.; Wiesener, M. S.; Chang, G. W.; Clifford, S. C.; Vaux, E. C.; Cockman, M. E.; Wykoff, C. C.; Pugh, C. W.; Maher, E. R.; Ratcliffe, P. J., The tumour suppressor protein VHL targets hypoxia-inducible factors for oxygen-dependent proteolysis. *Nature* **1999**, 399, (6733), 271-5.
37. Jaakkola, P.; Mole, D. R.; Tian, Y. M.; Wilson, M. I.; Gielbert, J.; Gaskell, S. J.; von Kriegsheim, A.; Hebestreit, H. F.; Mukherji, M.; Schofield, C. J.; Maxwell, P. H.; Pugh, C. W.; Ratcliffe, P. J., Targeting of HIF- α to the von Hippel-Lindau ubiquitylation complex by O₂-regulated prolyl hydroxylation. *Science* **2001**, 292, (5516), 468-72.
38. Lando, D.; Peet, D. J.; Whelan, D. A.; Gorman, J. J.; Whitelaw, M. L., Asparagine hydroxylation of the HIF transactivation domain a hypoxic switch. *Science* **2002**, 295, (5556), 858-61.
39. Lando, D.; Peet, D. J.; Gorman, J. J.; Whelan, D. A.; Whitelaw, M. L.; Bruick, R. K., FIH-1 is an asparaginyl hydroxylase enzyme that regulates the transcriptional activity of hypoxia-inducible factor. *Genes Dev* **2002**, 16, (12), 1466-71.
40. Schofield, C. J.; Ratcliffe, P. J., Oxygen sensing by HIF hydroxylases. *Nat Rev Mol Cell Biol* **2004**, 5, (5), 343-54.
41. Chan, D. A.; Sutphin, P. D.; Denko, N. C.; Giaccia, A. J., Role of prolyl hydroxylation in oncogenically stabilized hypoxia-inducible factor-1 α . *J Biol Chem* **2002**, 277, (42), 40112-7.
42. Kaluz, S.; Kaluzova, M.; Liao, S. Y.; Lerman, M.; Stanbridge, E. J., Transcriptional control of the tumor- and hypoxia-marker carbonic anhydrase 9: A one transcription factor (HIF-1) show? *Biochim Biophys Acta* **2009**, 1795, (2), 162-72.
43. Ivanov, S. V.; Kuzmin, I.; Wei, M. H.; Pack, S.; Geil, L.; Johnson, B. E.; Stanbridge, E. J.; Lerman, M. I., Down-regulation of transmembrane carbonic anhydrases in renal cell carcinoma cell lines by wild-type von Hippel-Lindau transgenes. *Proc Natl Acad Sci U S A* **1998**, 95, (21), 12596-601.
44. Kaluz, S.; Kaluzova, M.; Chrastina, A.; Olive, P. L.; Pastorekova, S.; Pastorek, J.; Lerman, M. I.; Stanbridge, E. J., Lowered oxygen tension induces expression of the hypoxia marker MN/carbonic anhydrase IX in the absence of hypoxia-inducible factor 1 α stabilization: a role for phosphatidylinositol 3'-kinase. *Cancer Res* **2002**, 62, (15), 4469-77.
45. Svastova, E.; Hulikova, A.; Rafajova, M.; Zat'ovicova, M.; Gibadulinova, A.; Casini, A.; Cecchi, A.; Scozzafava, A.; Supuran, C. T.; Pastorek, J.; Pastorekova, S., Hypoxia activates the capacity of tumor-associated carbonic anhydrase IX to acidify extracellular pH. *FEBS Lett* **2004**, 577, (3), 439-45.
46. Chiche, J.; Ilc, K.; Laferriere, J.; Trottier, E.; Dayan, F.; Mazure, N. M.; Brahimi-Horn, M. C.; Pouyssegur, J., Hypoxia-inducible carbonic anhydrase IX and XII promote tumor cell growth by counteracting acidosis through the regulation of the intracellular pH. *Cancer Res* **2009**, 69, (1), 358-68.
47. Vince, J. W.; Reithmeier, R. A., Carbonic anhydrase II binds to the carboxyl terminus of human band 3, the erythrocyte C1-/HCO₃⁻ exchanger. *J Biol Chem* **1998**, 273, (43), 28430-7.
48. Rout, M. P.; Aitchison, J. D., Pore relations: nuclear pore complexes and nucleocytoplasmic exchange. *Essays Biochem* **2000**, 36, 75-88.
49. Cronshaw, J. M.; Krutchinsky, A. N.; Zhang, W.; Chait, B. T.; Matunis, M. J., Proteomic analysis of the mammalian nuclear pore complex. *J Cell Biol* **2002**, 158, (5), 915-27.
50. Walde, S.; Kehlenbach, R. H., The Part and the Whole: functions of nucleoporins in nucleocytoplasmic transport. *Trends Cell Biol* **2010**, 20, (8), 461-9.
51. Andrade, M. A.; Petosa, C.; O'Donoghue, S. I.; Muller, C. W.; Bork, P., Comparison of ARM and HEAT protein repeats. *J Mol Biol* **2001**, 309, (1), 1-18.
52. Kalderon, D.; Richardson, W. D.; Markham, A. F.; Smith, A. E., Sequence requirements for nuclear location of simian virus 40 large-T antigen. *Nature* **1984**, 311, (5981), 33-8.
53. Dingwall, C.; Sharnick, S. V.; Laskey, R. A., A polypeptide domain that specifies migration of nucleoplasmin into the nucleus. *Cell* **1982**, 30, (2), 449-58.
54. Marg, A.; Shan, Y.; Meyer, T.; Meissner, T.; Brandenburg, M.; Vinkemeier, U., Nucleocytoplasmic shuttling by nucleoporins Nup153 and Nup214 and CRM1-dependent nuclear export control the subcellular distribution of latent Stat1. *J Cell Biol* **2004**, 165, (6), 823-33.

55. Cook, A.; Bono, F.; Jinek, M.; Conti, E., Structural biology of nucleocytoplasmic transport. *Annu Rev Biochem* **2007**, *76*, 647-71.
56. Chook, Y. M.; Blobel, G., Karyopherins and nuclear import. *Curr Opin Struct Biol* **2001**, *11*, (6), 703-15.
57. Sorokin, A. V.; Kim, E. R.; Ovchinnikov, L. P., Nucleocytoplasmic transport of proteins. *Biochemistry (Mosc)* **2007**, *72*, (13), 1439-57.
58. Pickart, C. M., Mechanisms underlying ubiquitination. *Annu Rev Biochem* **2001**, *70*, 503-33.
59. Chau, V.; Tobias, J. W.; Bachmair, A.; Marriott, D.; Ecker, D. J.; Gonda, D. K.; Varshavsky, A., A multiubiquitin chain is confined to specific lysine in a targeted short-lived protein. *Science* **1989**, *243*, (4898), 1576-83.
60. Pierce, N. W.; Kleiger, G.; Shan, S. O.; Deshaies, R. J., Detection of sequential polyubiquitylation on a millisecond timescale. *Nature* **2009**, *462*, (7273), 615-9.
61. Hershko, A.; Ciechanover, A., The ubiquitin system. *Annu Rev Biochem* **1998**, *67*, 425-79.
62. Deshaies, R. J., SCF and Cullin/Ring H2-based ubiquitin ligases. *Annu Rev Cell Dev Biol* **1999**, *15*, 435-67.
63. Lyapina, S.; Cope, G.; Shevchenko, A.; Serino, G.; Tsuge, T.; Zhou, C.; Wolf, D. A.; Wei, N.; Deshaies, R. J., Promotion of NEDD-CUL1 conjugate cleavage by COP9 signalosome. *Science* **2001**, *292*, (5520), 1382-5.
64. Goldenberg, S. J.; Cascio, T. C.; Shumway, S. D.; Garbutt, K. C.; Liu, J.; Xiong, Y.; Zheng, N., Structure of the Cand1-Cul1-Roc1 complex reveals regulatory mechanisms for the assembly of the multisubunit cullin-dependent ubiquitin ligases. *Cell* **2004**, *119*, (4), 517-28.
65. Liu, J.; Furukawa, M.; Matsumoto, T.; Xiong, Y., NEDD8 modification of CUL1 dissociates p120(CAND1), an inhibitor of CUL1-SKP1 binding and SCF ligases. *Mol Cell* **2002**, *10*, (6), 1511-8.
66. Bornstein, G.; Bloom, J.; Sitry-Shevah, D.; Nakayama, K.; Pagano, M.; Hershko, A., Role of the SCFSkp2 ubiquitin ligase in the degradation of p21Cip1 in S phase. *J Biol Chem* **2003**, *278*, (28), 25752-7.
67. Lee, J. E.; Sweredoski, M. J.; Graham, R. L.; Kolawa, N. J.; Smith, G. T.; Hess, S.; Deshaies, R. J., The steady-state repertoire of human SCF ubiquitin ligase complexes does not require ongoing Nedd8 conjugation. *Mol Cell Proteomics* **2011**, *10*, (5), M110 006460.
68. Martin, G. R., Isolation of a pluripotent cell line from early mouse embryos cultured in medium conditioned by teratocarcinoma stem cells. *Proc Natl Acad Sci U S A* **1981**, *78*, (12), 7634-8.
69. Evans, M. J.; Kaufman, M. H., Establishment in culture of pluripotential cells from mouse embryos. *Nature* **1981**, *292*, (5819), 154-6.
70. Bradley, A.; Evans, M.; Kaufman, M. H.; Robertson, E., Formation of germ-line chimaeras from embryo-derived teratocarcinoma cell lines. *Nature* **1984**, *309*, (5965), 255-6.
71. Smith, A. G., Embryo-derived stem cells: of mice and men. *Annu Rev Cell Dev Biol* **2001**, *17*, 435-62.
72. Keller, G. M., In vitro differentiation of embryonic stem cells. *Curr Opin Cell Biol* **1995**, *7*, (6), 862-9.
73. Niwa, H.; Miyazaki, J.; Smith, A. G., Quantitative expression of Oct-3/4 defines differentiation, dedifferentiation or self-renewal of ES cells. *Nat Genet* **2000**, *24*, (4), 372-6.
74. Chambers, I.; Colby, D.; Robertson, M.; Nichols, J.; Lee, S.; Tweedie, S.; Smith, A., Functional expression cloning of Nanog, a pluripotency sustaining factor in embryonic stem cells. *Cell* **2003**, *113*, (5), 643-55.
75. Avilion, A. A.; Nicolis, S. K.; Pevny, L. H.; Perez, L.; Vivian, N.; Lovell-Badge, R., Multipotent cell lineages in early mouse development depend on SOX2 function. *Genes Dev* **2003**, *17*, (1), 126-40.
76. Nichols, J.; Zevnik, B.; Anastassiadis, K.; Niwa, H.; Klewe-Nebenius, D.; Chambers, I.; Scholer, H.; Smith, A., Formation of pluripotent stem cells in the mammalian embryo depends on the POU transcription factor Oct4. *Cell* **1998**, *95*, (3), 379-91.

77. Chew, J. L.; Loh, Y. H.; Zhang, W.; Chen, X.; Tam, W. L.; Yeap, L. S.; Li, P.; Ang, Y. S.; Lim, B.; Robson, P.; Ng, H. H., Reciprocal transcriptional regulation of Pou5f1 and Sox2 via the Oct4/Sox2 complex in embryonic stem cells. *Mol Cell Biol* **2005**, 25, (14), 6031-46.
78. Ying, Q. L.; Nichols, J.; Chambers, I.; Smith, A., BMP induction of Id proteins suppresses differentiation and sustains embryonic stem cell self-renewal in collaboration with STAT3. *Cell* **2003**, 115, (3), 281-92.
79. Suzuki, A.; Raya, A.; Kawakami, Y.; Morita, M.; Matsui, T.; Nakashima, K.; Gage, F. H.; Rodriguez-Esteban, C.; Izpisua Belmonte, J. C., Nanog binds to Smad1 and blocks bone morphogenetic protein-induced differentiation of embryonic stem cells. *Proc Natl Acad Sci U S A* **2006**, 103, (27), 10294-9.
80. Doetschman, T. C.; Eistetter, H.; Katz, M.; Schmidt, W.; Kemler, R., The in vitro development of blastocyst-derived embryonic stem cell lines: formation of visceral yolk sac, blood islands and myocardium. *J Embryol Exp Morphol* **1985**, 87, 27-45.
81. Nakano, T.; Kodama, H.; Honjo, T., Generation of lymphohematopoietic cells from embryonic stem cells in culture. *Science* **1994**, 265, (5175), 1098-101.
82. Nishikawa, S. I.; Nishikawa, S.; Hirashima, M.; Matsuyoshi, N.; Kodama, H., Progressive lineage analysis by cell sorting and culture identifies FLK1+VE-cadherin+ cells at a diverging point of endothelial and hemopoietic lineages. *Development* **1998**, 125, (9), 1747-57.
83. Bain, G.; Kitchens, D.; Yao, M.; Huettner, J. E.; Gottlieb, D. I., Embryonic stem cells express neuronal properties in vitro. *Dev Biol* **1995**, 168, (2), 342-57.
84. Sucov, H. M.; Evans, R. M., Retinoic acid and retinoic acid receptors in development. *Mol Neurobiol* **1995**, 10, (2-3), 169-84.
85. Soprano, D. R.; Soprano, K. J., Retinoids as teratogens. *Annu Rev Nutr* **1995**, 15, 111-32.
86. Ying, Q. L.; Stavridis, M.; Griffiths, D.; Li, M.; Smith, A., Conversion of embryonic stem cells into neuroectodermal precursors in adherent monoculture. *Nat Biotechnol* **2003**, 21, (2), 183-6.
87. Tropepe, V.; Hitoshi, S.; Sirard, C.; Mak, T. W.; Rossant, J.; van der Kooy, D., Direct neural fate specification from embryonic stem cells: a primitive mammalian neural stem cell stage acquired through a default mechanism. *Neuron* **2001**, 30, (1), 65-78.
88. Lee, S. H.; Lumelsky, N.; Studer, L.; Auerbach, J. M.; McKay, R. D., Efficient generation of midbrain and hindbrain neurons from mouse embryonic stem cells. *Nat Biotechnol* **2000**, 18, (6), 675-9.
89. Watanabe, K.; Kamiya, D.; Nishiyama, A.; Katayama, T.; Nozaki, S.; Kawasaki, H.; Watanabe, Y.; Mizuseki, K.; Sasai, Y., Directed differentiation of telencephalic precursors from embryonic stem cells. *Nat Neurosci* **2005**, 8, (3), 288-96.
90. Parisi, S. E. A., A versatile method for differentiation of multiple neuronal subtypes from mouse embryonic stem cells. *J Stem Cells* **2007**, 1, 259-269.
91. Parisi, S.; Tarantino, C.; Paoletta, G.; Russo, T., A flexible method to study neuronal differentiation of mouse embryonic stem cells. *Neurochem Res* **2010**, 35, (12), 2218-25.
92. Presgraves, S. P.; Ahmed, T.; Borwege, S.; Joyce, J. N., Terminally differentiated SH-SY5Y cells provide a model system for studying neuroprotective effects of dopamine agonists. *Neurotox Res* **2004**, 5, (8), 579-98.
93. Melino, G.; Thiele, C. J.; Knight, R. A.; Piacentini, M., Retinoids and the control of growth/death decisions in human neuroblastoma cell lines. *J Neurooncol* **1997**, 31, (1-2), 65-83.
94. Lakso, M.; Vartiainen, S.; Moilanen, A. M.; Sirvio, J.; Thomas, J. H.; Nass, R.; Blakely, R. D.; Wong, G., Dopaminergic neuronal loss and motor deficits in *Caenorhabditis elegans* overexpressing human alpha-synuclein. *J Neurochem* **2003**, 86, (1), 165-72.
95. Link, C. D., Expression of human beta-amyloid peptide in transgenic *Caenorhabditis elegans*. *Proc Natl Acad Sci U S A* **1995**, 92, (20), 9368-72.
96. Jiang, H.; Guo, R.; Powell-Coffman, J. A., The *Caenorhabditis elegans* hif-1 gene encodes a bHLH-PAS protein that is required for adaptation to hypoxia. *Proc Natl Acad Sci U S A* **2001**, 98, (14), 7916-21.
97. Zhang, Y.; Shao, Z.; Zhai, Z.; Shen, C.; Powell-Coffman, J. A., The HIF-1 hypoxia-inducible factor modulates lifespan in *C. elegans*. *PLoS One* **2009**, 4, (7), e6348.

98. Mehta, R.; Steinkraus, K. A.; Sutphin, G. L.; Ramos, F. J.; Shamieh, L. S.; Huh, A.; Davis, C.; Chandler-Brown, D.; Kaerberlein, M., Proteasomal regulation of the hypoxic response modulates aging in *C. elegans*. *Science* **2009**, 324, (5931), 1196-8.
99. Chen, D.; Thomas, E. L.; Kapahi, P., HIF-1 modulates dietary restriction-mediated lifespan extension via IRE-1 in *Caenorhabditis elegans*. *PLoS Genet* **2009**, 5, (5), e1000486.
100. Budde, M. W.; Roth, M. B., Hydrogen sulfide increases hypoxia-inducible factor-1 activity independently of von Hippel-Lindau tumor suppressor-1 in *C. elegans*. *Mol Biol Cell* **2010**, 21, (1), 212-7.
101. Bellier, A.; Chen, C. S.; Kao, C. Y.; Cinar, H. N.; Aroian, R. V., Hypoxia and the hypoxic response pathway protect against pore-forming toxins in *C. elegans*. *PLoS Pathog* **2009**, 5, (12), e1000689.
102. Shen, C.; Nettleton, D.; Jiang, M.; Kim, S. K.; Powell-Coffman, J. A., Roles of the HIF-1 hypoxia-inducible factor during hypoxia response in *Caenorhabditis elegans*. *J Biol Chem* **2005**, 280, (21), 20580-8.
103. Pocock, R.; Hobert, O., Oxygen levels affect axon guidance and neuronal migration in *Caenorhabditis elegans*. *Nat Neurosci* **2008**, 11, (8), 894-900.
104. Padilla, P. A.; Nystul, T. G.; Zager, R. A.; Johnson, A. C.; Roth, M. B., Dephosphorylation of cell cycle-regulated proteins correlates with anoxia-induced suspended animation in *Caenorhabditis elegans*. *Mol Biol Cell* **2002**, 13, (5), 1473-83.
105. Nystul, T. G.; Goldmark, J. P.; Padilla, P. A.; Roth, M. B., Suspended animation in *C. elegans* requires the spindle checkpoint. *Science* **2003**, 302, (5647), 1038-41.
106. Hajeri, V. A.; Trejo, J.; Padilla, P. A., Characterization of sub-nuclear changes in *Caenorhabditis elegans* embryos exposed to brief, intermediate and long-term anoxia to analyze anoxia-induced cell cycle arrest. *BMC Cell Biol* **2005**, 6, 47.
107. Hajeri, V. A.; Stewart, A. M.; Moore, L. L.; Padilla, P. A., Genetic analysis of the spindle checkpoint genes *san-1*, *mdf-2*, *bub-3* and the CENP-F homologues *hcp-1* and *hcp-2* in *Caenorhabditis elegans*. *Cell Div* **2008**, 3, 6.
108. Edghill-Smith, Y.; Bray, M.; Whitehouse, C. A.; Miller, D.; Mucker, E.; Manischewitz, J.; King, L. R.; Robert-Guroff, M.; Hryniewicz, A.; Venzon, D.; Meseda, C.; Weir, J.; Nalca, A.; Livingston, V.; Wells, J.; Lewis, M. G.; Huggins, J.; Zwiers, S. H.; Golding, H.; Franchini, G., Smallpox vaccine does not protect macaques with AIDS from a lethal monkeypox virus challenge. *J Infect Dis* **2005**, 191, (3), 372-81.
109. Scott, B. A.; Avidan, M. S.; Crowder, C. M., Regulation of hypoxic death in *C. elegans* by the insulin/IGF receptor homolog DAF-2. *Science* **2002**, 296, (5577), 2388-91.
110. Mendenhall, A. R.; LaRue, B.; Padilla, P. A., Glyceraldehyde-3-phosphate dehydrogenase mediates anoxia response and survival in *Caenorhabditis elegans*. *Genetics* **2006**, 174, (3), 1173-87.
111. Fasseas, M. K.; Tsikou, D.; Flemetakis, E.; Katinakis, P., Molecular and biochemical analysis of the alpha class carbonic anhydrases in *Caenorhabditis elegans*. *Mol Biol Rep* **2011**, 38, (3), 1777-85.
112. Bishop, T.; Lau, K. W.; Epstein, A. C.; Kim, S. K.; Jiang, M.; O'Rourke, D.; Pugh, C. W.; Gleadle, J. M.; Taylor, M. S.; Hodgkin, J.; Ratcliffe, P. J., Genetic analysis of pathways regulated by the von Hippel-Lindau tumor suppressor in *Caenorhabditis elegans*. *PLoS Biol* **2004**, 2, (10), e289.
113. Hall, R. A.; Vullo, D.; Innocenti, A.; Scozzafava, A.; Supuran, C. T.; Klappa, P.; Muhlschlegel, F. A., External pH influences the transcriptional profile of the carbonic anhydrase, CAH-4b in *Caenorhabditis elegans*. *Mol Biochem Parasitol* **2008**, 161, (2), 140-9.
114. Giacomotto, J.; Pertl, C.; Borrel, C.; Walter, M. C.; Bulst, S.; Johnsen, B.; Baillie, D. L.; Lochmuller, H.; Thirion, C.; Segalat, L., Evaluation of the therapeutic potential of carbonic anhydrase inhibitors in two animal models of dystrophin deficient muscular dystrophy. *Hum Mol Genet* **2009**, 18, (21), 4089-101.
115. Sherman, T. A.; Rongali, S. C.; Matthews, T. A.; Pfeiffer, J.; Nehrke, K., Identification of a nuclear carbonic anhydrase in *Caenorhabditis elegans*. *Biochim Biophys Acta* **2012**, 1823, (4), 808-17.

116. Encinas, M.; Iglesias, M.; Liu, Y.; Wang, H.; Muhaisen, A.; Cena, V.; Gallego, C.; Comella, J. X., Sequential treatment of SH-SY5Y cells with retinoic acid and brain-derived neurotrophic factor gives rise to fully differentiated, neurotrophic factor-dependent, human neuron-like cells. *J Neurochem* **2000**, *75*, (3), 991-1003.
117. Bell, S. P.; Learned, R. M.; Jantzen, H. M.; Tjian, R., Functional cooperativity between transcription factors UBF1 and SL1 mediates human ribosomal RNA synthesis. *Science* **1988**, *241*, (4870), 1192-7.
118. Pan, P. W.; Parkkila, A. K.; Autio, S.; Hilvo, M.; Sormunen, R.; Pastorekova, S.; Pastorek, J.; Haapasalo, H.; Parkkila, S., Brain phenotype of carbonic anhydrase IX-deficient mice. *Transgenic Res* **2012**, *21*, (1), 163-76.
119. Steinhoff, A.; Pientka, F. K.; Mockel, S.; Kettelhake, A.; Hartmann, E.; Kohler, M.; Depping, R., Cellular oxygen sensing: Importins and exportins are mediators of intracellular localisation of prolyl-4-hydroxylases PHD1 and PHD2. *Biochem Biophys Res Commun* **2009**, *387*, (4), 705-11.
120. Mylonis, I.; Chachami, G.; Samiotaki, M.; Panayotou, G.; Paraskeva, E.; Kalousi, A.; Georgatsou, E.; Bonanou, S.; Simos, G., Identification of MAPK phosphorylation sites and their role in the localization and activity of hypoxia-inducible factor-1alpha. *J Biol Chem* **2006**, *281*, (44), 33095-106.
121. Groulx, I.; Lee, S., Oxygen-dependent ubiquitination and degradation of hypoxia-inducible factor requires nuclear-cytoplasmic trafficking of the von Hippel-Lindau tumor suppressor protein. *Mol Cell Biol* **2002**, *22*, (15), 5319-36.
122. Koritzinsky, M.; Wouters, B. G., Hypoxia and regulation of messenger RNA translation. *Methods Enzymol* **2007**, *435*, 247-73.
123. Janiszewska, M.; De Vito, C.; Le Bitoux, M. A.; Fusco, C.; Stamenkovic, I., Transportin regulates nuclear import of CD44. *J Biol Chem* **2010**, *285*, (40), 30548-57.
124. Giri, D. K.; Ali-Seyed, M.; Li, L. Y.; Lee, D. F.; Ling, P.; Bartholomeusz, G.; Wang, S. C.; Hung, M. C., Endosomal transport of ErbB-2: mechanism for nuclear entry of the cell surface receptor. *Mol Cell Biol* **2005**, *25*, (24), 11005-18.
125. Bryant, D. M.; Stow, J. L., Nuclear translocation of cell-surface receptors: lessons from fibroblast growth factor. *Traffic* **2005**, *6*, (10), 947-54.
126. Caratu, G.; Allegra, D.; Bimonte, M.; Schiattarella, G. G.; D'Ambrosio, C.; Scaloni, A.; Napolitano, M.; Russo, T.; Zambrano, N., Identification of the ligands of protein interaction domains through a functional approach. *Mol Cell Proteomics* **2007**, *6*, (2), 333-45.